Normal Nearby Galaxies[*]

Marc Sauvage[1], Richard J. Tuffs[2], Cristina C. Popescu[2]

[1] *CEA/DSM/DAPNIA/Service d'Astrophysique,*
C.E. Saclay, 91191 Gif sur Yvette CEDEX, France
Email:msauvage@cea.fr
[2] *Max Planck Institut für Kernphysik, Astrophysics Department,*
Saupfercheckweg 1, 69117 Heidelberg, Germany,
Email: Richard.Tuffs@mpi-hd.mpg.de
Cristina.Popescu@mpi-hd.mpg.de

Abstract. Following on from IRAS, ISO has provided a huge advancement in our knowledge of the phenomenology of the infrared (IR) emission of normal galaxies and the underlying physical processes. Highlights include: the discovery of an extended cold dust emission component, present in all types of gas-rich galaxies and carrying the bulk of the dust luminosity; the definitive characterisation of the spectral energy distribution in the IR, revealing the channels through which stars power the IR light; the derivation of realistic geometries for stars and dust from ISO imaging; the discovery of cold dust associated with HI extending beyond the optical body of galaxies; the remarkable similarity of the near-IR (NIR)/ mid-IR (MIR) SEDs for spiral galaxies, revealing the importance of the photo-dissociation regions in the energy budget for that wavelength range; the importance of the emission from the central regions in shaping up the intensity and the colour of the global MIR luminosity; the discovery of the "hot" NIR continuum emission component of interstellar dust; the predominance of the diffuse cold neutral medium as the origin for the main interstellar cooling line, [CII] 158 μm, in normal galaxies.

1. Introduction

Whereas IRAS provided the first systematic survey of infrared (IR) emission from normal galaxies, it has been the photometric, imaging and spectroscopic capabilities of ISO (Kessler et al., 1996; Kessler et al., 2003) which have unravelled the basic physical processes giving rise to this IR emission. Thanks to the broad spectral grasp of ISO, the bulk of the emission from dust could be measured, providing the first quantitative assessment of the fraction of stellar light re-radiated by dust. The battery of filters has led to a definitive characterisation of the spectral energy distribution (SED) in the IR, revealing the contribution of the

---

[*] Based on observations with ISO, an ESA project with instruments funded by ESA Member States (especially the PI countries: France, Germany, the Netherlands and the United Kingdom) and with the participation of ISAS and NASA.

different stellar populations in powering the IR emission. The imaging capabilities have unveiled the complex morphology of galaxies in the IR, and their changing appearance with IR wavelength. They also allowed the exploration of hitherto undetected faint diffuse regions of galaxies. The contribution of different grain populations to the emission has been measured through their characteristic spectroscopic signatures. Knowledge of the emission from cooling lines of the interstellar medium (ISM) has been extended to low luminosity quiescent spiral and dwarf galaxies.

In this review we will concentrate on the mid-IR (MIR) to far-IR (FIR) properties of normal nearby galaxies. By normal we essentially mean that their SEDs are not powered by accretion. We will begin with spiral galaxies, since these have attracted most of the ISO observers' attention. From these objects we will move to the other class of gas-rich galaxies, the dwarfs. However, as the nearby extragalactic population is not only made of spirals and dwarfs, we will conclude by the exploring the very varied IR properties of early-type galaxies.

2. Spiral Galaxies

2.1. SPATIAL DISTRIBUTIONS

2.1.1. *FIR Morphologies*
ISOPHOT (Lemke et al., 1996; Laureijs et al., 2003) imaged three nearby galaxies (M 31: Haas et al. 1998; M 33: Hippelein et al. 2003 and M 101: Tuffs & Gabriel 2003) in the 60 to $200\,\mu$m range, with sufficient linear resolution to easily distinguish between the main morphological components in the FIR - nucleus, spiral arms and underlying disk. The main discovery, made possible by the unprecedented surface brightness sensitivity longwards of $100\,\mu$m, was the existence of large amounts of cold dust associated both with the spiral arms and with the underlying disk. This dust was too cold to have been seen by IRAS. Furthermore, ground-based submillimeter (submm) facilities lacked the surface brightness sensitivity to map the diffuse component of the cold dust associated with the underlying disk, though they detected the component associated with the spiral arms (e.g. Bianchi et al. 2000b).

In the case of the Sab galaxy M 31, most of the emission at $170\,\mu$m arises from the underlying disk, which has a completely diffuse appearance (Fig. 1, left panel). This diffuse disk emission can be traced out to a radius of $22\,$kpc, so the galaxy has a similar overall size in the FIR as seen in the optical bands. Fig. 1 (left panel) also shows that at $170\,\mu$m the spiral arm component is dominated by a ring of
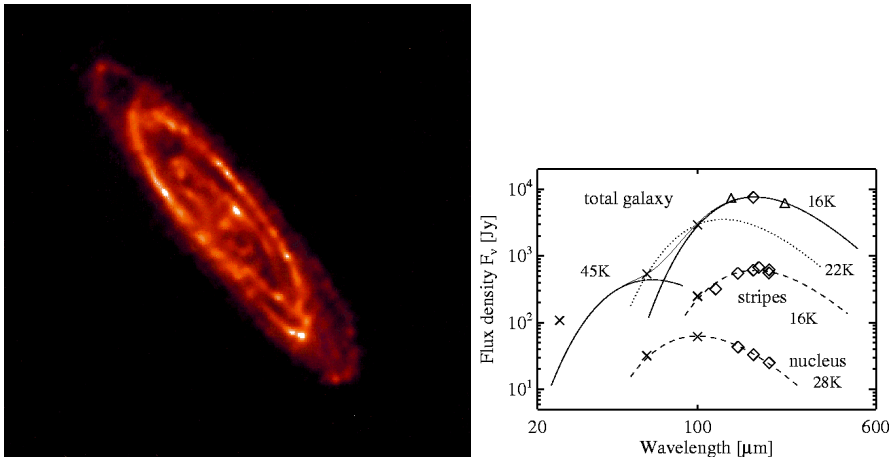
Figure 1. Left: ISOPHOT 170 μm map of M 31 (Haas et al. 1998), with an angular resolution of 1.3′. North is towards the top, and East is towards the left. The field size is 2.9 × 2.9 degrees. Right: Infrared SED of M 31 (Haas et al. 1998). The data are shown by symbols (diamonds ISO, crosses IRAS, triangles DIRBE) with the size being larger than the errors. The blackbody curves with emissivity proportional to λ^{-2} are shown by lines. The dotted line with T=22 K through the IRAS 60 and 100 μm data points indicates what one would extrapolate from this wavelength range alone without any further assumptions.

10 kpc radius. In addition, there is a faint nuclear source, which is seen more prominently in HIRES IRAS 60 μm maps at similar resolution and in Hα. The overall SED (Fig. 1, right panel) can be well described as a superposition of two modified (β=2) Planck curves, with dust temperatures T_{D} of 16 and 45 K. The cold dust component at 16 K arises from both the ring structure (30%) and the diffuse disk (70%; Haas, private communication), illustrating the importance of the diffuse emission at least for this example. The 45 K component matches up well with H\textsc{ii} regions within the star-formation complexes in the ring structure. Associated with each star-formation complex are also compact, cold emission sources (see Fig. 3 of Schmitobreick et al., 2000) with dust temperatures in the 15 to 20 K range. These could well represent the parent molecular clouds in the star-formation complexes which gave rise to the H\textsc{ii} regions. Detailed examination of the morphology of the ring shows a smooth component of cold dust emission as well as the discrete cold dust sources. Finally, the nuclear emission was fitted by a 28 K dust component.

   The ISOPHOT maps of the Sc galaxies M 33 and M 101 show the same morphological components as seen in M 31, with the difference that the spiral arm structure can be better defined in these later-

type spirals. Also the star-formation complexes in the spiral arms show similar SEDs to those seen in M 31.

In conclusion, the characteristics of the FIR emission from the main morphological components of spiral galaxies are:

- **nucleus**: an unresolved warm source with $T_D \sim 30\,\mathrm{K}$

- **spiral arms**: a superposition of:

  - localised warm emission with $40 \leq T_D \leq 60\,\mathrm{K}$ from HII regions
  - localised cold emission with $15 \leq T_D \leq 20\,\mathrm{K}$ from parent molecular clouds
  - diffuse emission running along the arms

- **disk**: an underlying diffuse (predominantly cold) emission with $12 \leq T_D \leq 20\,\mathrm{K}$
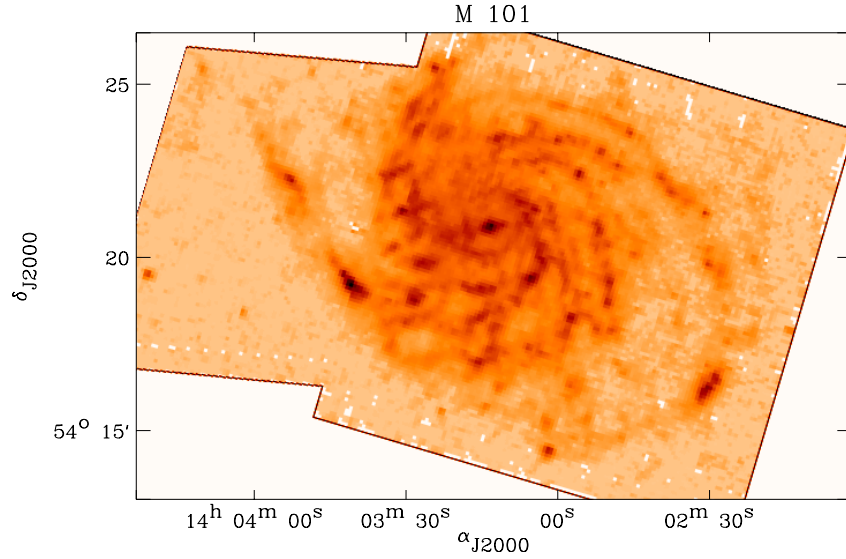
2.1.2. *MIR Morphologies*

Generally, ISOCAM (Cesarsky et al., 1996; Blommaert et al., 2003) maps of nearby galaxies are difficult to compare with their FIR counterparts from ISOPHOT, for two reasons. On the one hand ISOCAM's far superior angular resolution enables the mapping of detailed structures even within the spiral arm. On the other hand ISOPHOT's surface brightness sensitivity is far superior to that of ISOCAM, enabling faint diffuse emission on scales of galactic disks to be traced. ISOCAM's smaller PSF also meant that different galaxies were generally mapped in the MIR than in the FIR. M 31 and M 33 were too large to be completely mapped with ISOCAM.

Observations of a portion of the southern disk of M 31 were presented by Pagani et al. (1999). Due to the vastly different scales, these observations are particularly difficult to relate to those of Haas et al. (1998) but they nevertheless reveal that the detected MIR emission originates mostly in the regions of the spiral arms of Fig. 1. In fact, M 31 was completely mapped by Kraemer et al. (2002) at a number of MIR wavelengths with the *Midcourse Space Experiment* and their $8.3\,\mu\mathrm{m}$ map (their Fig. 1) is strikingly similar to that of Haas et al. (1998), with the difference that the diffuse emission detected in the FIR beyond the main spiral arms is not detected in the MIR. This difference could for instance be understood as being due to different parts of the grain size distribution having different spatial extents. However, generalising such a conclusion on the basis of the observation of M 31 alone could

be dangerous, as it is known that some of the dust properties of this galaxy are very different from those of other galaxies, as revealed by it's atypical MIR spectrum (Cesarsky et al., 1998).

A better grasp of the MIR morphology of spiral galaxies can be obtained from studies that completely mapped their targets. Such studies were predominantly made in the 6.75 and 15 μm broad band filters of ISOCAM (occasionally the ISOCAM 12 μm filter was used). These filters were chosen to trace different components of the MIR emission in galaxies. The 6.7 μm filter includes the most prominent spectral features emitted by Polycyclic Aromatic Hydrocarbons (PAHs) powered by UV photons, as revealed by spectroscopic studies of galactic sources. The 15 μm filter was originally chosen to trace stochastic emission from very small grains, though it subsequently turned out that PAH emission from the 12.7 μm feature and an underlying PAH continuum can also contribute and even dominate the signal seen towards the spiral arms. Morphological studies made using the above mentioned filters were presented by Malhotra et al. (1996) for NGC 6946, by Smith (1998) for NGC 7331, by Sauvage et al. (1996) for M 51 as well as by Bendo et al. (2002a), Dale et al. (2000) and Roussel et al. (2001c) for larger samples of spiral galaxies. These papers show that, in the MIR, spiral galaxies present a morphology that is quite similar to that observed at other optical/NIR wavelengths. The spiral arms are very prominent, with the giant HII region complexes showing up as emission enhancements along the arms. A diffuse underlying MIR emitting disk is often detected in the interarm regions of the inner disk. Finally, a central region of varying importance is observed. A clear example of these morphological features is given in Fig. 2 where the 6.75 μm map of M 101 from Roussel et al. (2001c) is presented. Although the central region of spiral galaxies is generally dominated optically by the bulge of old stars, one should not jump to the conclusion that the central MIR component is dominated by the Rayleigh-Jeans emission of cold photospheres or circumstellar envelopes. The extent of the central MIR source is generally different from that of the stellar bulge and furthermore Roussel et al. (2001b) showed that its IR colours are generally not those expected from stars (i.e. the 15/6.75 μm flux ratio is generally larger than unity whereas the opposite applies in early-type galaxies where the stars provide most of the 6.75 μm emission, see Athey et al., 2002 or Xilouris et al., 2004, and Fig. 9). In fact, most of the emission from the central regions of spiral galaxies can be attributed to dust emission powered by enhanced star formation (Roussel et al., 2001b).

A further detailed study of the morphological features in the MIR is the multiwavelength study of M 83 by Vogler et al. (2004) who present the azimuthally averaged radial profiles of a number of emission com-

Figure 2. The $6.75\,\mu$m map of M 101, from Roussel et al. (2001c). The different features of the MIR morphology, central region, H II regions, spiral arms, are clearly seen. Diffuse interarm emission is also present but it becomes rapidly too faint to be detected.

ponents of the galaxy. These profiles show that the MIR emission of M 83 can be decomposed into a central component, associated with the central starburst, the prominent arm structure and a diffuse exponentially fading disk emission. The arm/interarm contrast was found to be larger in the MIR than it is in the optical, although it was found to be smaller than what is observed in Hα. This was interpreted as being again due to the important, if not dominant role of star-formation in powering the MIR emission, through the generation of UV photons. The fact that particles responsible for the MIR emission can be excited by a broad range of photon energies (see e.g. Uchida et al., 2000 and Li & Draine, 2002) explains why the influence of star-forming regions is seen on broader scales than the actual extent of H II regions (see also Sect. 2.2.2).

An obvious question arising from these investigations pertains to the colour of the various MIR emission components (central regions, spiral arms, interarm regions), which could potentially be used to reveal the heating sources of MIR emission. Searches made in this direction came up with mixed results. For instance Sauvage et al. (1996) reported a systematic variation of the $15/6.75\,\mu$m flux ratio along some cuts through the arms of M 51, while Helou et al. (1996) showed that, on average, the

15/6.75 μm flux ratio is the same for the arm and interarm regions of NGC 6946, and Smith (1998) reported no systematic spectral variations in the disk of NGC 7331. The only systematic colour variations are observed in the central regions of spiral galaxies, where the 15/6.75 μm flux ratio can reach values observed in starburst galaxies (Roussel et al., 2001b). Another study of the physical interpretation of the MIR morphology of spiral galaxies was presented by Dale et al. (1999). This shows that although star-formation activity is the primary driver for surface brightness variations inside galaxies, it is only for regions of intense activity that a colour variation occurs. Column density also appears as a secondary parameter to explain the difference in disk surface brightness between galaxies.

This relatively fast exploration of the IR morphology of spiral galaxies thus reveals how the same processes that affect their visible shapes, i.e. intensity and distribution of star-forming regions, play an important part in determining their IR aspect. It already suggests that the MIR and FIR part of the spectrum behave differently, in the sense that spectral modifications are more apparent in the FIR than in the MIR. This is not unexpected given the different thermodynamical states of the grains that produce these emissions, thermal equilibrium for most of the FIR, and stochastic heating for most of the MIR.

2.1.3. *The extent of spiral disks in the FIR*

Further information about the true distribution of dust in spiral disks is provided by FIR observations of galaxies more distant than the highly resolved local galaxies discussed in Sect. 2.1.1, but still close enough to resolve the diffuse disk at the longest FIR wavelengths accessible to ISO. In a study of eight spiral galaxies mapped by ISOPHOT at 200 μm, Alton et al. (1998; see also Davies et al. 1999 for NGC 6946) showed that the observed scalelength of FIR emission at 200 μm is greater than that found by IRAS at 60 and 100 μm. Thus, the scalelength of the FIR emission increases with increasing FIR wavelength. This result was reinforced using LWS (Clegg et al., 1996; Gry et al., 2003) measurements of the dust continuum by Trewhella et al. (2000), and can also be inferred from Fig. 2 of Hippelein et al. (2003) for M 33. We note here that this implies that the bulk of the 200 μm emission arises from grains heated by a radially decreasing radiation field, as would be expected for grains in the diffuse disk. If most of the 200 μm emission had arisen from localised sources associated with the parent molecular clouds within the spiral arms, there should be no FIR colour gradient in the galaxy, since the SEDs of the localised sources should not depend strongly on position.

The second result to come out of the studies by Alton et al. (1998) and Davies et al. (1999) is that the observed scalelength at $200\,\mu$m is comparable to or exceeds the scalelength of the optical emission (see also Tuffs et al. 1996). As noted by Alton et al., this result implies that the *intrinsic* scalelength of the dust in galaxies is greater than that of the stars. This is because the apparent scalelength of stars should increase with increasing disk opacity (since the inner disk is expected to be more opaque than the outer disk) whereas the apparent scalelength of the dust emission will be less than the intrinsic scalelength (due to the decrease in grain temperature with increasing galactocentric radius). The extraction of the precise relation between the intrinsic scalelengths of stars and dust requires a self-consistent calculation of the transfer of radiation through the disk (see Sect. 2.3). The reason for the difference between the intrinsic scalelength of stars and dust in galaxies is not self-evident, since it is the stars themselves which are thought to be the sources of interstellar grains (produced either in the winds of evolved intermediate mass stars or perhaps in supernovae). One might speculate either that there is a mechanism to transport grains from the inner disk to the outer disk, or that the typical lifetimes of grains against destruction by shocks is longer in the outer disk than it is in the inner disk.

While Alton et al. and Davies et al. showed that the scalelength of the $200\,\mu$m emission was comparable to or slightly larger than that of the optical emission, these studies did not actually detect grain emission beyond the edge of the optical disk. Since spiral galaxies in the local universe are commonly observed to be embedded in extended disks of neutral hydrogen - the so called "extended HI disks", it is a natural question to ask whether these gaseous disks contain grains. This question was answered in the affirmative by Popescu & Tuffs (2003), through dedicated deep FIR maps of a large field encompassing the entire HI disk of the edge-on spiral galaxy NGC 891, made using ISOPHOT at 170 and $200\,\mu$m (see Fig. 3).

The large amounts of grains found in the extended HI disk (gas-to-dust ratio of $\sim 1\%$) clearly shows that this gaseous disk is not primordial, left over from the epoch of galaxy formation. It was suggested that the detected grains could have either been transported from the optical disk (via the halo, using mechanisms such as those proposed by Ferrara (1991), Davies et al. (1998), Popescu et al. (2000a) or through the action of macro turbulence) or that they could have been produced outside the galaxy (for example transferred in interactions with other galaxies). It is interesting to note that, although the dust emission is seen towards the HI component, the grains may not actually be embedded in the neutral ISM. Instead, this dust could
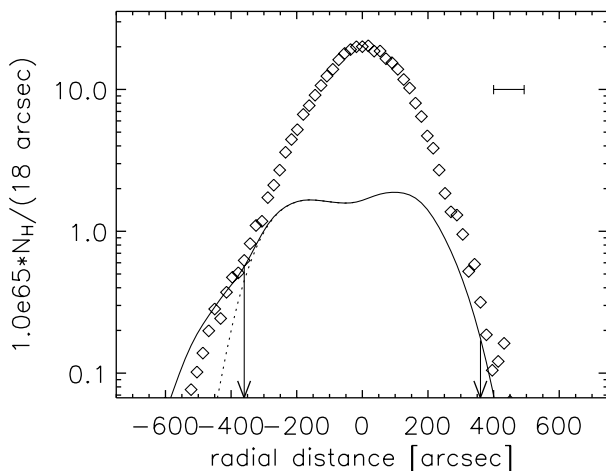
Figure 3. The radial profiles of Hɪ emission (from Swaters et al. 1997) convolved with the ISOPHOT PSF (solid line) and of $200\,\mu m$ FIR emission (symbols) of NGC 891 (Popescu & Tuffs 2003). Note that the extent and asymmetry of the $200\,\mu m$ emission follow that of the HI emission. The profiles are sampled at intervals of $18''$. The negative radii correspond to the southern side of the galaxy and the galaxy was scanned at 60 degrees with respect to the major axis. The units of the FIR profile are W/Hz/pixel, multiplied by a factor of 2×10^{-22} and the error bars are smaller than the symbols. The horizontal bar delineates the FWHM of the ISOPHOT PSF of $93''$. The vertical arrows indicate the maximum extent of the optically emitting disk. The dotted line represents a modified Hɪ profile obtained in the southern side from the original one by cutting off its emission at the edge of the optical disk and by convolving it with the ISOPHOT PSF.

trace an "unseen" molecular component, as proposed by Pfenniger & Combes (1994), Pfenniger, Combes & Martinet (1994), Gerhard & Silk (1996), and Valentijn & van der Werf (1999b). This cold molecular gas component has been invoked as a dark matter component to explain the flat rotation curves of spiral galaxies. Its presence might also reconcile the apparent discrepancy between the very low metallicities measured in Hɪɪ regions in the outer disk (Ferguson, Gallagher & Wyse 1998) and the high ratio of dust to gas (on the assumption that all gas is in form of HI) found by Popescu & Tuffs (2003) in the extended Hɪ disk of NGC 891.

2.1.4. *The extent of spiral disks in the MIR*
As alluded to in the discussion of the MIR aspect of M 31 above, the MIR disks of spiral galaxies are generally quite short. At first glance they can even appear truncated since in the outer region the emission is generally dominated by the Hɪɪ regions of the arms, superimposed on a very diffuse disk emission. This appearance is however mostly an "optical" illusion. The radial profiles of the exponentially declining

MIR disk emission of M 83 Vogler et al. (2004) show a scalelength that is clearly shorter than that seen in any optical bands, but with no truncation. The strong decrease of star-formation activity in the outer regions of galaxies induces a rapid disappearance of the MIR emission, although, as is definitely revealed by long-wavelength observations, dust is still present at large galactocentric distances.

A more systematic study of the extent of MIR spiral disks was presented in Roussel et al. (2001c). These authors have defined a MIR disk diameter, D_{MIR}, in a similar way as the definition used in the optical, by measuring the diameter of the $5\,\mu Jy/arcsec^{-2}$ isophote at $6.75\,\mu m$ (this is roughly the detection limit of this band). This definition allows to compare optical and MIR diameters on a broad range of galaxies. It shows that the IR diameter (as defined above) is systematically smaller than the optical one (the largest value of D_{MIR}/D_{opt} observed in this sample of about 70 galaxies is slightly less than 1, while the smallest value observed is $\sim$0.3). The variation of D_{MIR}/D_{opt} can be related to both the morphological type of the galaxies or their H I deficiency in the sense that earlier type or more severely H I deficient galaxies have a smaller D_{MIR}/D_{opt}. Roussel et al. (2001c) indicate that the H I deficiency is likely the dominant parameter given that H I-deficient galaxies are often classified as early-type galaxies, due to the absence of star-forming regions at large galactocentric distances. The MIR diameter of a galaxy is thus essentially determined by the extent of the star-forming activity through its disk, demonstrating the crucial role of star-formation in powering the MIR emission.

The fact that the MIR disks appear so much smaller than the FIR disks immediately prompts the following question: does the dust responsible for the MIR emission disappear at large galactocentric distances, or phrased differently, should we observe a MIR counterpart to the FIR extended distributions? As mentioned before, ISOCAM was probably less sensitive than ISOPHOT to faint diffuse emission, which would bias the ISOCAM maps toward small-scale bright structures such as the H II regions in the disks. This would explain why MIR emission is not detected far out in the disk, but still leaves open the question of why the scalelength of the MIR emission is so much shorter than that of the FIR emission.

2.1.5. *Comparison with morphologies at other wavelengths*

Comparison with the optical
Although one immediately associates IR light with dust, the fact that ISO could reach relatively short IR wavelengths prompts the question of the contribution of stars to the shortest ISO bands. And indeed,
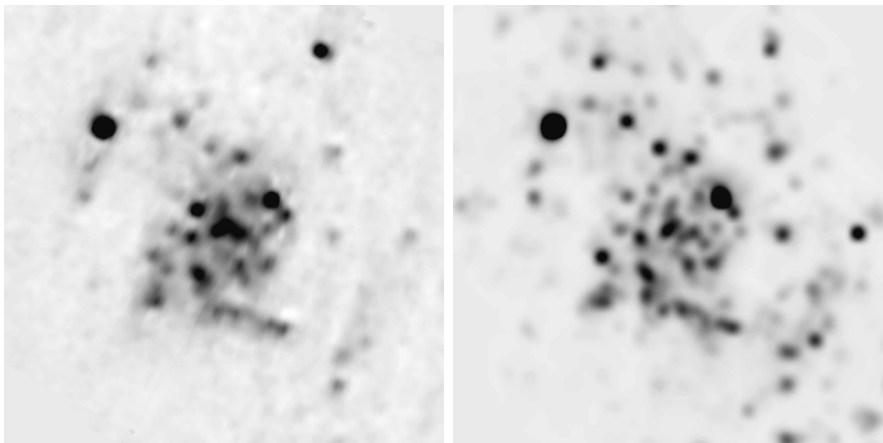
Figure 4. Left: Distribution of the localised warm dust component at 60 μm, F_{60}^l, in M 33 (Hippelein et al 2003). This is the scaled difference map $2(F_{60} - 0.165 \times F_{160})$, with the factor 0.165 given by the average flux density ratio F_{60}/F_{170} in the interarm regions. Right: $H\alpha$ map of M 33 convolved to a resolution of 60$''$.

when studied quantitatively through the use of light concentration indices, as done for instance by Boselli et al. (2003b), the morphology of galaxies at MIR and NIR wavelengths show surprising similarities. This indicates at least a similar spatial distribution of dust and stars, which is not too surprising given the origin of the MIR emission (see later). However, determining the actual contribution of stellar photospheres and circumstellar shells to the ISO fluxes is harder, as it requires first the construction of a pure stellar image and second the correct extrapolation in wavelength of this image to the ISO wavelengths, taking into account the possible stellar population gradients in the galaxy. This type of work led Boselli et al. (2003a) to conclude that a large fraction of the 6.75 μm flux in galaxies could be due to stars, ranging from 80 % in Sa to 20 % in Sc galaxies. This conclusion is however not supported by the analysis of Lu et al. (2003) who showed that already at 6 μm, the mean flux of their galaxies is one order of magnitude larger than what is observed in galaxies devoid of interstellar medium (see Fig. 9). Therefore it appears unlikely that stars make a large contribution to the IR emission of spiral galaxies longwards of 6 μm, even though the spatial distribution of the emission shares some morphological properties with that of the stars, a fact which is due to their common link with the star-formation process.

Comparison with Hα

For the highly resolved galaxy M 33, Hippelein et al. (2003) showed that there is a strong resemblance between the morphology of the localised
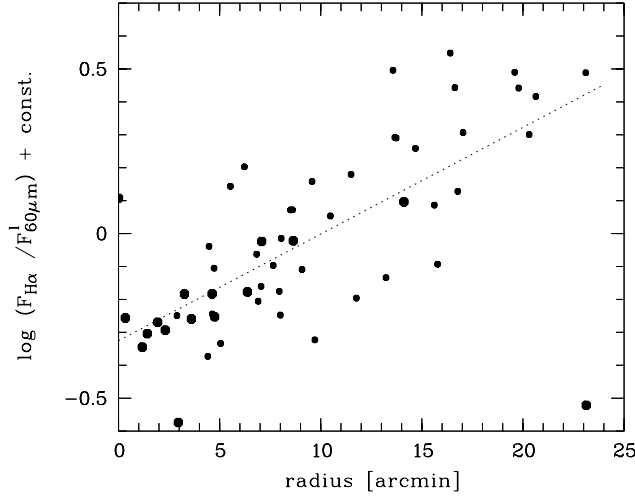
Figure 5. The ratio of $F_{H\alpha}$ to the localised warm dust component at $60\,\mu$m, $F_{60}^{\rm l}$, for the star-forming regions in M 33 (Hippelein et al. 2003) versus distance from the galaxy centre. Symbol sizes indicate the brightness of the sources.

warm dust component at $60\,\mu$m ($F_{60}^{\rm l}$; obtained at each direction by subtracting the $170\,\mu$m map scaled by the ratio of the $60/170\,\mu$m brightness in the interarm regions) and the morphology of the Hα emission (see Fig. 4), indicating that the $60\,\mu$m localised emission traces the star-formation complexes. The $F_{H\alpha}/F_{60}^{\rm l}$ ratio (see Fig. 5) for the star-formation complexes shows a clear systematic increase with increasing radial distance from the centre (allowing for the [NII] line contribution decreasing with distance, the slope would be even steeper). Very probably this is due to the presence of a larger scale gradient of opacity affecting the recombination line fluxes.

Similarly, in the MIR a number of authors have noted a striking resemblance between MIR and Hα maps of galaxies, which should not come as a surprise given the numerous links between MIR emission and star-formation mentioned above. This is both the case for the well studied galaxies M 51 (Sauvage et al., 1996), NGC 7331 (Smith, 1998), M 83 (Vogler et al., 2004) and NGC 6946 (Walsh et al., 2002) and for larger samples of more distant objects (see for instance Contursi et al., 2001 or Domingue et al., 2003). However, few authors have studied the relation between the two emissions *within* galaxies. Sauvage et al. (1996) presented a comparison of the MIR/Hα ratio for a number of H$_{\rm II}$ region complexes in M 51. This reveals that extinction affecting the measure of Hα is responsible for most of the variation observed in the MIR/Hα ratio.

One should note that the apparently strong spatial correlation between the MIR and Hα maps is slightly misleading, in the sense that the limited spatial resolution tends to make the maps more similar than they really are. Studies of resolved Hɪɪ regions indeed show that the MIR emission tends to avoid the peaks of Hα emission and rather delineates the edges of molecular clouds exposed to the radiation produced by newly-formed stars (see e.g. Contursi et al., 1998 or Contursi et al., 2000 and Fig. 8).

The complexity of the local relation between the MIR emission and Hα is revealed by the studies of Vogler et al. (2004) and Walsh et al. (2002). Using maps at the same resolution, and only taking independent points, these authors showed that the local MIR-Hα correlation is quite poor and highly non-linear. As we will see, this is in contrast to the global MIR-Hα correlation, which is linear and tighter. A plausible explanation of this, first introduced in the context of the FIR emission by Popescu et al. (2002; see also Pierini et al. 2003b), would be the existence of a diffuse component of the MIR emission from the underlying disk, powered by the star-formation activity, but on larger scales than that used by Walsh et al. (2002) or Vogler et al. (2004).

Comparison with UV

A fundamental property of spiral galaxies is the fraction of light from young stars which is re-radiated by dust. This property can be investigated as a function of position in the galaxy by a direct comparison of ISOPHOT maps at 60, 100 and 170 μm with UV maps obtained with GALEX (Galaxy Evolution Explorer; Martin et al. 2005) in its near-UV (NUV; 2310 Å) and far-UV (FUV; 1530 Å) bands. Such a comparison was performed for M 101 by Popescu et al. (2005). The top panels in Fig. 6 display the 100 μm ISOPHOT image (left) together with the corresponding "total UV" (integrated from 1412 to 2718 Å) image (right). Comparison between the ratio image (100 μm/UV) (bottom left panel) and an image of the "spiral arm fraction" (the fraction of the UV emission from the spiral arm within an ISOPHOT beam; bottom right panel) shows that the high values of the 100 μm/UV ratio trace the interarm regions. In other words the "spiral features" in the ratio image are in reality regions of diffuse emission which are interspaced with the real spiral features, as seen in the "spiral arm fraction" image.

The trend for the FIR/UV ratio to be higher in the diffuse interarm regions than in the spiral-arms is seen in Fig. 7 from the segregation of the blue dots and red diamonds at a given radius. This apparently surprising result was explained in terms of the escape probability of UV photons from spiral arms and their subsequent scattering in the interarm regions, and in terms of the larger relative contribution of
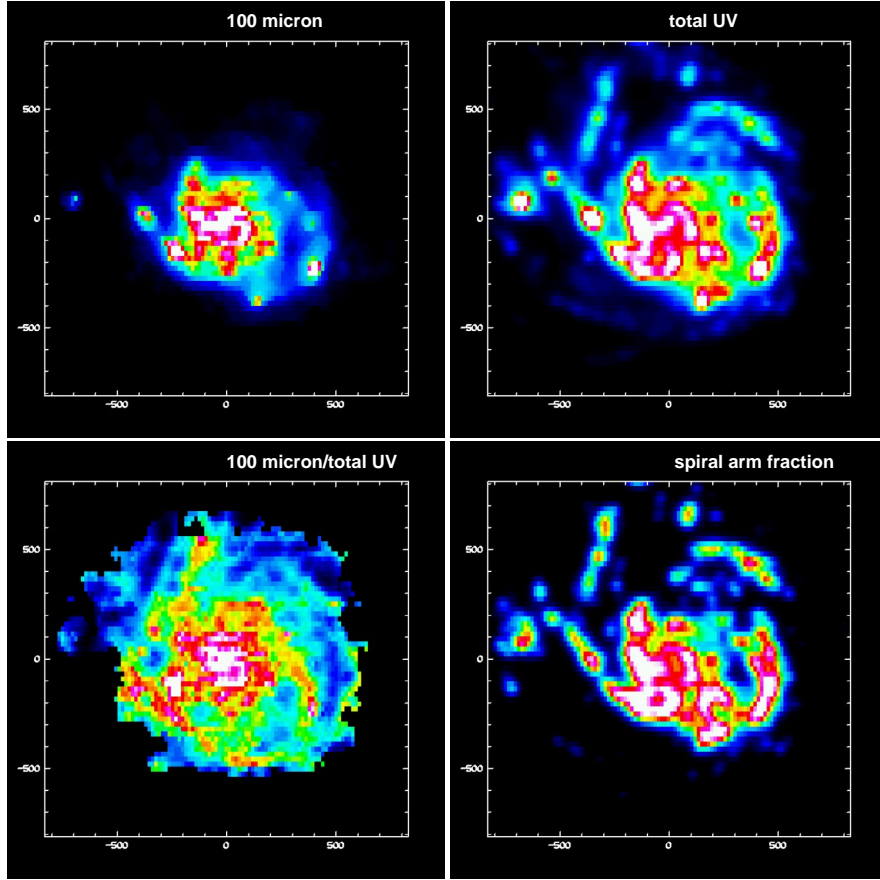
Figure 6. FIR-UV comparison for M 101 (Popescu et al. 2005). Top left panel: filter-integrated $100\,\mu$m ISOPHOT image. Top right panel: "total UV" image converted to the orientation, resolution and sampling of the $100\,\mu$m ISOPHOT image. Bottom left panel: the ratio image of the filter-integrated $100\,\mu$m ISOPHOT image divided by the corresponding "total UV" image. Bottom right panel: the image of the "spiral arm fraction" at the orientation, resolution and sampling of the $100\,\mu$m ISOPHOT image. All panels depict a field of $27.7' \times 27.1'$ centered at $\alpha^{2000} = 14^{\mathrm{h}}03^{\mathrm{m}}13.11^{\mathrm{s}}$; $\delta^{2000} = 54°21'06.6''$. The pixel size is $15.33'' \times 23.00''$.

optical photons to the heating of the dust in the interarm regions. The combined effect of the optical heating and the scattering of the UV emission means that the FIR/UV ratio will not be a good indicator of extinction in the interarm region.

Despite these local variations, the main result of Popescu et al. (2005) is the discovery of a tight dependence of the FIR/UV ratio on radius, with values monotonically decreasing from ~ 4 in the nuclear region to nearly zero towards the edge of the optical disk (see Fig. 7). This was interpreted in terms of the presence of a large-scale distri-
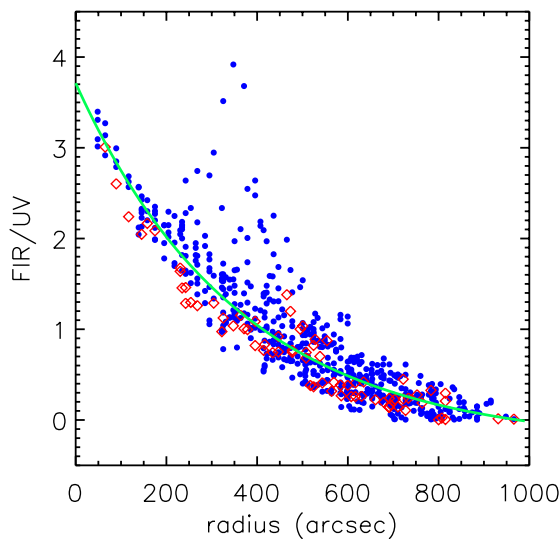
Figure 7. The pixel values of the FIR/UV ratio map of M 101 (Popescu et al. 2005) at the resolution of the 170 μm image versus angular radius. The blue dots are for lines of sight towards interarm regions and the red diamonds towards the spiral arm regions. The green solid line is an offset exponential fit to the data.

bution of diffuse dust having a face-on optical depth which decreases with radius and which dominates over the more localised variations in opacity between the arm and interarm regions.

A comparison of the UV and MIR morphologies, analogous to the UV-FIR comparison for M 101, has been made for the south-west ring of M 31 by Pagani et al. (1999). Here the 20″ resolution 200 nm map from the FOCA 1000 balloon experiment is compared to the ~ 6″ resolution 6.75 μm ISOCAM map (Fig. 8). This study, and especially its Fig. 8, shows that although the overall morphology of the two maps appears similar, following the ring-like structure observed in that region of the galaxy, the UV and MIR emission actually complement each other: UV-emitting regions fill the holes in the distribution of the 6.75 μm emission. In fact, the same study shows a much tighter spatial correlation of the MIR emission with the gaseous components (Hi or CO) than with the UV emission. Again, this is interpreted as showing that even if most of the energy that ultimately powers the MIR emission is generated in the giant HII region complexes that are seen in Hα or UV light, most of the MIR emission comes from the surfaces of the molecular clouds that *surround* these complexes.

These differences in the UV and MIR spatial distribution are confirmed by the recent observations of the Spitzer satellite, which also reveal that at 24 μm the association between IR and UV or Hα emission
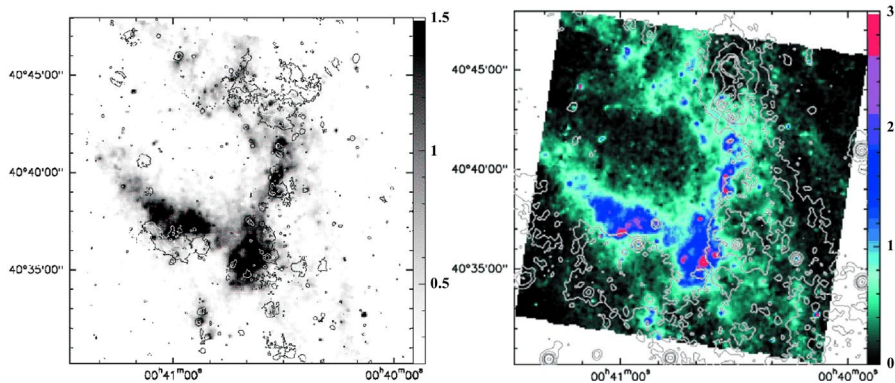
Figure 8. The SW ring of M 31 observed by Pagani et al. (1999). On the left panel, Hα contours in black are superimposed on a grey scale map at $6.75\,\mu$m. On the right panel, UV contours are superposed on the same map, in colour this time. In both maps, though the overall ring-like structure is preserved at all wavelengths, it is clear that the UV and Hα emissions tend to be located in regions of minimal $6.75\,\mu$m emission, and that reversely, the MIR emission is located on the edges of the Hα and UV regions.

becomes tighter, even at high spatial resolution (Helou et al., 2004). The reason for this will be elucidated in section 2.2.2.

2.2. INTEGRATED PROPERTIES

The overriding result of all ISOPHOT studies of the integrated properties of normal galaxies in the FIR is that their SEDs in the 40-200 μm spectral range require both warm and cold dust emission components to be fitted. Although the concept of warm and cold emission components is as old as IRAS (de Jong et al. 1984), it only became possible to directly measure and spectrally separate these components using ISOPHOT's multi-filter coverage of the FIR regime out to 200 μm.

In the MIR the two most stunning results are the high similarity of the disk's SED in spiral galaxies and the almost complete invariance of the global MIR colours to the actual star-formation activity of the galaxy as a whole. The former result shows that the MIR emission comes predominantly from PDRs, whereas the latter result demonstrates the importance of the emission from the central region to the MIR, a characteristic which could only be uncovered due to the high spatial resolution offered by ISOCAM.

In order to investigate the integrated properties of local universe gas-rich galaxies, a number of statistical samples were constructed, which were primarily observed by ISOPHOT and ISOCAM. All these projects

were complementary in terms of selection and observational goals. In descending order of depth (measured in terms of a typical bolometric luminosity of the detected objects), the published surveys are:

The ISO Virgo Cluster Survey is a combination of the ISOPHOT Virgo Cluster Deep Survey (IVCDS; Tuffs et al. 2002a,b; Popescu et al. 2002) and ISOCAM measurements (Boselli et al., 2003b, see also Boselli et al., 1997) of the same sample supplemented by additional targets on the eastern side of the cluster. The IVCDS represents the *deepest survey* (both in luminosity and surface brightness terms) of normal galaxies measured in the FIR with ISO. A complete volume- and luminosity-limited sample of 63 gas-rich Virgo Cluster galaxies selected from the Virgo Cluster Catalogue (Binggeli et al. 1985; see also Binggeli et al. 1993) with Hubble types later than S0 and brighter than $B_\mathrm{T} \leq 16.8$ were mapped with ISOPHOT at 60, 100 and $170\,\mu\mathrm{m}$. A total of 99 galaxies were mapped with ISOCAM in the 6.7 and $15\,\mu\mathrm{m}$ filters. The IVCDS sample was (in part) also observed with the LWS (Leech et al. 1999).

The ISO Virgo Cluster Survey provides a database for statistical investigations of the FIR and MIR SEDs of gas-rich galaxies in the local universe spanning a broad range in star-formation activity and morphological types, including dwarf systems and galaxies with rather quiescent star-formation activity.

The Coma/A1367 Survey (Contursi et al., 2001) consists of 6 spiral and 12 irregular galaxies having IRAS detections at $60\,\mu\mathrm{m}$. The galaxies were selected to be located within 2 or 1 degrees of the X-ray centres of Coma and A1367 clusters, respectively, with emphasis on peculiar optical morphologies. Each galaxy was observed in a single pointing with ISOPHOT, at 120, 170 and $200\,\mu\mathrm{m}$, as well as mapped with ISOCAM in the 6.75 and $15\,\mu\mathrm{m}$ broadband filters. The sample provides a database of integrated flux densities for a pure cluster sample of high luminosity spiral and irregular galaxies.

The ISO Bright Spiral Galaxies Survey (Bendo et al. 2002a,b; 2003) consists of 77 spiral and S0 galaxies chosen from the Revised Shapley-Ames Catalog (RSA), with $B_\mathrm{T} \leq 12.0$. Almost all are IRAS sources. Mainly an ISOCAM mapping survey with the $12\,\mu\mathrm{m}$ filter, the project also used ISOPHOT to take 60, 100 and $170\,\mu\mathrm{m}$ short stares towards the nucleus of the galaxies and towards background fields. The sample provides a database of MIR morphologies and FIR surface brightnesses of the central regions of bright spiral galaxies, including S0s.

The ISO Bright Spiral Galaxies Survey and the ISO Virgo Cluster Survey represent the principle investigations of optically selected samples of normal galaxies. It should be emphasised that the main

difference between them is primarily one of shallow versus deep, rather than field versus cluster, since by design the Virgo Sample predominantly consists of infalling galaxies from the field, and no cluster specific effects could be found (see also Contursi et al. for Coma/A1367 Sample).

The ISO Key Project on Normal Galaxies Sample (Dale et al., 2000) consists of 69 galaxies selected to span the whole range of the classical IRAS colour-colour diagram (Helou, 1986). Since IRAS detected a vast number of galaxies in its four bands, the selection was also made to span the Hubble sequence evenly and provide a broad range of IR luminosities, dust temperatures (as determined by IRAS) and star-formation activity. Galaxies in the sample were mapped with ISOCAM, their main cooling lines in the FIR were measured with ISOLWS (Malhotra et al., 2001) and their 2.5-12 μm spectra were measured with ISOPHOT-S (Lu et al., 2003).

The ISOCAM Parallel Mode Survey (Ott et al., 2003) is drawn from observations made with ISOCAM, mostly around 6 μm, while another ISO instrument was prime. It detected around 16000 distinct objects down to 0.5 mJy. Identifications of these objects by cross-correlation with other catalogues is on-going and $\sim$25% of the objects are expected to be galaxies.

The ISOPHOT Serendipity Survey (Stickel et al. 2000) has initially catalogued 115 galaxies with $S_\nu \geq 2$ Jy at 170 μm and with morphological types predominantly S0/a - Scd. This sample provides a database of integrated 170 μm flux densities for relatively high luminosity spiral galaxies, all detected by IRAS at 60 & 100 μm. Recently a catalogue of 1900 galaxies was released (Stickel et al. 2004), of which a small fraction does not have IRAS detections. Most of the 1900 galaxies are spirals. The measured 170 μm flux densities range from just below 0.5 Jy up to ~ 600 Jy.

Finally about 30 additional spiral galaxies were mapped in various ISO guaranteed and open time programs (see Roussel et al., 2001c, for a compilation)

2.2.1. *The FIR spectral energy distribution: Dust temperatures,*
       masses and luminosities

The presence of a cold dust emission component peaking longwards of 120 μm was inferred from studies of the integrated SEDs of individual galaxies (see Sect. 2.1.1), from statistical studies of small samples (Krügel et al. 1998; Siebenmorgen et al. 1999) and was confirmed and generalised by studies of the larger statistical samples mentioned above. The latter studies also demonstrated the universality of the cold dust component, showing it to be present within all types of spirals (Tuffs

& Popescu 2003). The cold emission component predominantly arises from dust heated by the general diffuse interstellar medium and the warm component from locally heated dust in HII regions, an interpretation consistent with what has been seen in the ISOPHOT maps of nearby galaxies (see Sect. 2.1.1) and with self-consistent modelling of the UV-FIR SEDs (see Sect. 2.3).

The cold dust component is most prominent in the most "quiescent" galaxies, like those contained in the IVCD sample, where the cold dust temperatures were found to be broadly distributed, with a median of $18\,\mathrm{K}$ (Popescu et al. 2002), some $8 - 10\,\mathrm{K}$ lower than would have been predicted by IRAS. The corresponding dust masses were correspondingly found to be increased by factors of typically $2 - 10$ (Stickel et al. 2000) for the Serendipity Sample and by factors $6 - 13$ (Popescu et al. 2002) for the IVCD sample, with respect to previous IRAS determinations. As a consequence, the derived gas-to-dust ratios are much closer to the canonical value of ~ 160 for the Milky Way (Stickel et al. 2000, Contursi et al. 2001; see also Haas et al. 1998 for M 31), but with a broad distribution of values (Popescu et al. 2002).

It was found that the cold dust component provides not only the bulk of the dust masses, but even the bulk of the FIR luminosity, in particular for the case of the most quiescent spirals, like those in the IVCD sample. In contrast to the SEDs found by the other ISOPHOT studies, which typically peaked at around $170\,\mu\mathrm{m}$, Bendo et al. (2003) derived spatially integrated SEDs typically peaking at around $100\,\mu\mathrm{m}$. The result of Bendo et al. may reflect the fact that these observations were single pointings, made towards the nucleus of resolved galaxies extending (in the main) beyond the field of view of ISOPHOT, and were therefore biased towards nuclear emission, which is warmer than the extended cold dust emission missed (or only partially covered) by these measurements. Nevertheless, the measurements of Bendo et al. constitute a useful probe of the FIR emission of the inner disks. This emission (normalised to K band emission) was found to increase along the Hubble sequence (Bendo et al. 2002b).

Since the FIR carries most of the dust luminosity, it is interesting to re-evaluate the question of the fraction of stellar photons converted via grains into IR photons, taking into account the comprehensive measurements of the cold dust emission component made available by ISOPHOT. This was done by Popescu & Tuffs (2002a), who showed that the mean percentage of stellar light reradiated by dust is $\sim 30\%$ for the Virgo Cluster spirals contained in the IVCD sample. This study also included the dust emission radiated in the NIR-MIR range. The fact that the mean value of $\sim 30\%$ found for the Virgo Cluster spirals is the same as the canonical value obtained for the IRAS Bright Galaxy

Sample (BGS; Soifer & Neugebauer 1991) is at first sight strange, since IRAS was not sensitive to the cold dust component. However the BGS sample is an IR selected sample and biased towards galaxies with higher dust luminosities, while the Virgo sample is optically selected and contain a full representation of quiescent systems. So the deficit in FIR emission caused by sample selection criteria for the Virgo sample is compensated for by the inclusion of the cold dust component. Popescu & Tuffs (2002a) also found evidence for an increase of the ratio of the dust emission to the total stellar emitted output along the Hubble sequence, ranging from typical values of $\sim 15\%$ for early spirals to up to $\sim 50\%$ for some late spirals. This trend was confirmed by Boselli et al. (2003a) who further utilised the new ISO data on dust emission to constrain the corresponding absorption of starlight and thus improve extinction corrections (using the technique pioneered by Xu & Buat 1995 for the IRAS data).

2.2.2. *The NIR to MIR spectral energy distribution*

Using the large body of NIR-MIR data - both photometric and spectroscopic - from the statistical studies mentioned previously, one can also determine the general properties of the SED of galaxies from the NIR to the MIR.

Concerning the colours of galaxies in the MIR, the main property that is evidenced is a remarkable uniformity of the $6.75/15\,\mu$m flux ratio. In contrast with the well-known IRAS colour-colour diagram, the composite ISO-IRAS colour diagram (showing the $6.75/15\,\mu$m flux ratio versus the $60/100\,\mu$m flux ratio, see Dale et al., 2000) shows a plateau of the $6.75/15\,\mu$m flux ratio for a large range of $60/100\,\mu$m flux ratios. A decrease of the ISO colour is only observed for the largest values of the IRAS colour. A rapid interpretation of that behaviour is that for most galaxies, the ISOCAM filters collect emission from transiently heated PAHs which shows no spectral dependence on the heating intensity. It is only for the most actively star-forming galaxies that a fraction of the $15\,\mu$m flux originates in hot dust located in the Hɪɪ regions. This simple interpretation has to be taken with caution since it assumes that the integrated colour reflects a global property of the object (e.g. its star-forming activity). Indeed, following up on the fact that in the MIR the central regions of spiral galaxies appear to differ from the disk (see Sect. 2.1.2), Roussel et al. (2001b) inspected the behaviour of the $6.75/15\,\mu$m flux ratio separately for disks and central regions. This revealed that the disk colours are extremely similar from one galaxy to the other and that it is the fraction of the total flux emitted from the central region combined with the colour of that region that dominate the variation of the global $6.75/15\,\mu$m flux ratio, rather than the global
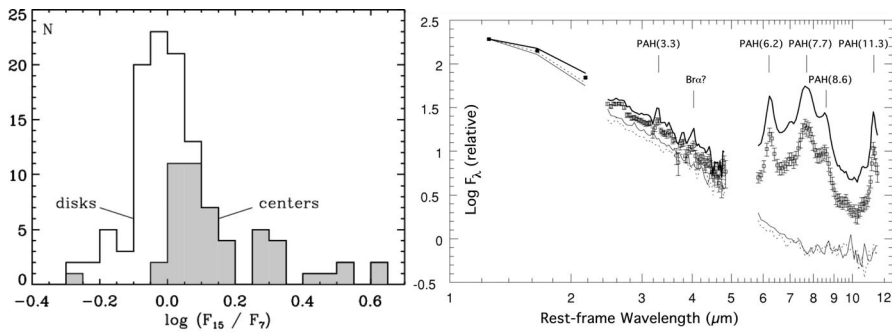
Figure 9. On the left panel, we show the distribution of 15/6.75 μm flux ratio for the disks and central regions of spiral galaxies (taken from Roussel et al., 2001b). It is clear that the disks have a very uniform colour while the central regions explore a much larger range. On the left side, the global NIR-MIR SED (from Lu et al., 2003) reveals the dominance of the PAH features in the MIR, as well as the very small dispersion from one object or the other. Both PAH dominated spectra represent the average spectrum of the sample, with two different normalisation. The very small dispersion bars reveal the homogeneity of the sample. The thin solid and dotted lines are spectra from early-type galaxies, dominated by stars.

level of star-formation activity (Fig. 9). We remark that, in principle, the decrease of the 6.75/15 μm flux ratio in the central regions could correspond to a drop of the 6.75 μm flux rather than to an increase of the 15 μm flux. That this is not the case is clearly demonstrated by the ISOCAM spectra of these central regions (Roussel et al., 2001b) that show the appearance of the expected small grains continuum at the long wavelength edge of the bandpass.

This uniformity of the disk emission is confirmed by the spectroscopic study of Lu et al. (2003). With the spectroscopic capabilities of ISOPHOT-S, they showed that the 2.5-12 μm spectrum of spiral galaxies is indeed extremely uniform. The NIR part is dominated by the tail of photospheric emission, while the MIR part presents the classical features of PAH emission, with extremely small spectral variations of these features from one galaxy to the other (of the order of 20%, see Fig. 9). Furthermore, these variations are not related to the IRAS 60/100 μm colour or to the FIR-to-blue luminosity ratio. Thus, as revealed by the broad-band colours, it appears that the detailed SED of spiral galaxies in the MIR show very little dependence on the actual level of star-formation in the galaxy. Studies of the MIR SED of various regions in our own galaxies have shown that a spectrum such as that observed globally in spiral galaxies is prototypical of photo-dissociation regions (PDRs), e.g. the outer layers of molecular clouds exposed to moderately strong radiation fields (see e.g. van Dishoeck,

2004). Hence the spatial distribution of the MIR emission revealed in Sect. 2.1 is fully consistent with the observed SED.

It should be noted, however, that the ISOPHOT-S spectral range is shorter than the one explored by the $15\,\mu$m filter of ISOCAM, and in fact covers a wavelength range that is not very sensitive spectrally to activity variations, as demonstrated by the study of starburst galaxies presented by Förster-Schreiber et al. (2003). Therefore it is from the combination of the nearly constant colours observed by Roussel et al. (2001b) and the constant spectrum observed by Lu et al. (2003) that one can conclude that the 5-18 μm spectrum of galactic disks is dominated by the emission from PDRs, rather than from the HII regions themselves.

The systematic exploration of the NIR-MIR SED of spiral galaxies made possible by ISO offered a number of other important discoveries. First Lu et al. (2003) evidenced a new component of dust emission consisting of a "hot" NIR continuum emission. Its association with the ISM was made clear by the existence of a correlation between that NIR excess and the strength of the PAH features. However a physical explanation of this continuum is still lacking. Second, the strength of the PAH emission (which represents most, but not all of the MIR flux when defined as the 5-20 μm luminosity for instance), was found to be well correlated spatially with the 850 μm flux of bright regions inside a number of galaxies (Haas et al., 2002). This can be interpreted as showing a close physical association between cold dust clouds and the PAHs, but, given the limited spatial resolutions involved, more likely indicates that the localised 850 μm emission comes essentially from the inside of the molecular clouds whose surfaces produce the PAH features. Finally Helou et al. (2001) found a strong correlation between the 5-10 μm luminosity and the [CII] line luminosities of actively star-forming galaxies from the sample of Malhotra (2001). Since the [CII] emission from this sample mainly originates in PDRs (see Sect. 2.4.1), this correlation implies that PAHs, which dominate the 5-10 μm luminosities (Lu et al., 2003), are also responsible for most of the gas heating in strongly star-forming galaxies.

2.2.3. *Two outstanding questions of the IRAS era*

The radio-FIR correlation

One of the most surprising discoveries of the IRAS all-sky survey was the very tight and universal correlation between the spatially integrated FIR and radio continuum emissions (de Jong et al. 1985; Helou et al. 1985; Wunderlich et al. 1987; see Völk & Xu 1994 for a review). However all the pre-ISO studies of the FIR/radio correlation were based on FIR luminosities derived from the IRAS 60 and 100 μm flux densi-
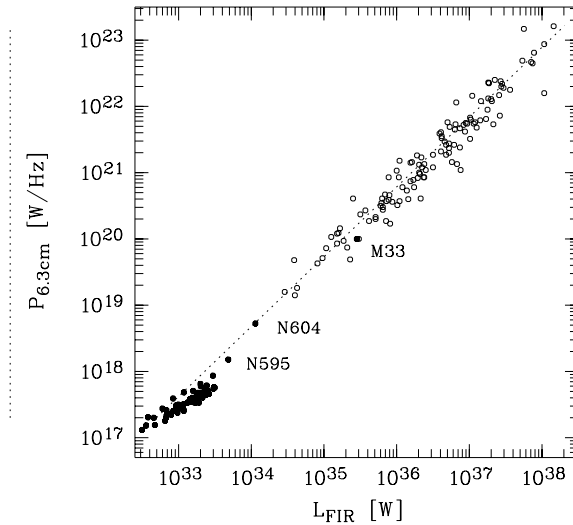
Figure 10. Plot of the monochromatic radio luminosity versus the FIR luminosities for M 33 (Hippelein et al. 2003) and its star-forming regions (filled circles) together with the data for the Effelsberg 100-m galaxy sample (Wunderlich et al. 1987, open circle). The dotted line has a slope of 1.10 (Wunderlich & Klein 1988).

ties, and thus were missing the bulk of the cold dust luminosity. The ISOPHOT measurements at 60, 100 and 170 μm were used to redefined the FIR/radio correlation (Pierini et al. 2003b) for a statistical sample of spiral galaxies. The inclusion of the cold dust component was found to produce a tendency for the total FIR/radio correlation to become more non-linear than inferred from the IRAS 60 and 100 μm observations. The use of the three FIR wavelengths also meant that, for the first time, the correlation could be directly derived for the warm and cold dust emission components. The cold FIR/radio correlation was found to be slightly non-linear, whereas the warm FIR/radio correlation is linear. Because the effect of disk opacity in galaxies would introduce a non-linearity in the cold-FIR/radio correlation, in the opposite sense to that observed, it was argued that both the radio and the FIR emissions are likely to have a non-linear dependence on SFR. For the radio emission an enhancement of the small free-free component with SFR can account for this effect. For the cold FIR emission a detailed analysis of the dependence of local absorption and opacity of the diffuse medium on SFR is required to understand the non-linear trend of the correlation (see Pierini et al. 2003b).

The improved angular resolution of ISO compared with IRAS also allowed a more detailed examination of the local FIR-radio correlation on sub-kpc size galactic substructures. Hippelein et al. (2003) established the correlation for the star-forming regions in M 33. This correlation is

shown in Fig 10, overplotted on the correlation for integrated emission from galaxies. It is apparent that the local correlation has a shallower slope (of the order of 0.9) than for the global correlation. It was argued that the local correlation is attributable to the increase with SFR of dust absorption in increased dust densities, and to local synchrotron emission from within supernova remnants, still confining their accelerated electrons. Both emission components play only a minor role in the well known global radio-FIR correlation, that depends on the dominant large-scale absorption/re-emission properties of galaxies.

This local correlation has also been investigated in the MIR by Vogler et al. (2004). A good correlation was found between the two emissions on scales of $\sim 500\,\mathrm{pc}$, which is comparable to the scales of the individual regions considered for the local FIR-radio correlation in M 33. The slope of the local MIR-radio correlation was comparable to that of the local FIR-radio correlation. This is consistent with the MIR and FIR emissions on scales of $\sim 500\,\mathrm{pc}$ being powered by the same UV photons.

Infrared emission as a star-formation tracer

Because star-forming regions and Hii complexes shine brightly in the IR, and because starburst galaxies output most of their energy in the IR, this wavelength domain has always been associated with star-formation. As we have seen earlier, this is supported by a qualitative analysis of the IR emission of galaxies, but a quantitative assessment of this association has proven difficult. With the enhanced capacities of ISO, this question has been addressed in much more detail, and this reveals that the different regions of the IR SED have a different link with star-formation.

In the FIR, the correlation with the most widely-used star-formation tracer, Hα, is extremely non-linear, which has long led authors to suspect that the FIR emission is the result of more than one component (see e.g. Lonsdale-Persson & Helou, 1987). With ISOPHOT the correlation was separately established for the warm and cold dust emission components. A good linear correlation was found between the warm FIR luminosities (normalised to the K band luminosity) derived for the IVCD sample and their Hα EW (Popescu et al. 2002). This is in agreement with the assumption that the warm dust component is mainly associated with dust locally heated within star-formation complexes. The scatter in the correlation was attributed to a small component of warm emission from the diffuse disk (produced either by transiently heated grains or by grains heated by old stellar population), as well as to the likely variation in HII region dust temperatures within and between galaxies. A good but non-linear correlation was found between the cold
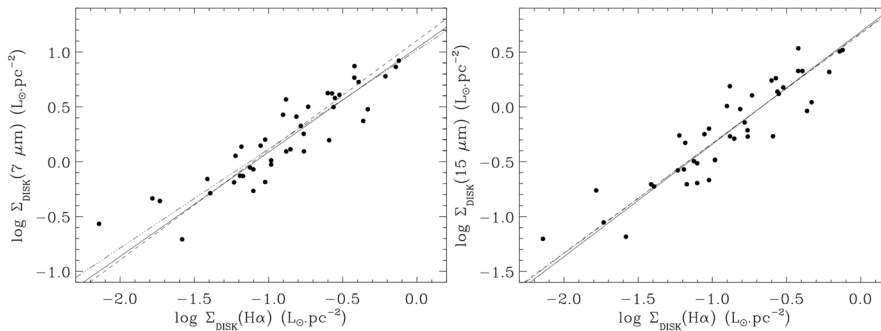
Figure 11. The MIR-Hα correlation for the disks of spiral galaxies (adapted from Roussel et al., 2001a). Here only the disk fraction of the MIR flux is used, and the Hα fluxes are uniformly corrected for 1 magnitude of extinction. All fluxes are normalised by the galaxy size to remove size-related biases. For both fluxes the correlation is extremely linear. Lines on the graphs correspond to different adjustment methods, but all give a slope very close to unity.

FIR luminosities of the galaxies from the IVCD sample and their Hα EW, in the sense that FIR increases more slowly than Hα. Since the bulk of the cold FIR emission arises from the diffuse disk, the existence of this correlation implies that the grains in the diffuse disk are mainly powered by the UV photons (see also Sect. 2.3). The non-linearity of the correlation is consistent with there being a higher contribution from optical photons in heating the grains in more quiescent galaxies.

For the late-type galaxies in the Coma and A1367 clusters, Contursi et al. (2001) derived the relationships between the IR flux densities at 200, 170, 120, 100 and $60\,\mu$m, normalised to the H band flux, as a function of the Hα EW. It was found that the poorer correlation is in the $200\,\mu$m band and that the values of the fitted slopes decrease as the FIR wavelength increases. These results should be interpreted in terms of the increasing contribution of the diffuse component with increasing FIR wavelength.

Using the ISOPHOT observations from Tuffs et al. (2002a,b) and Stickel et al. (2000) in combination with UV and K band photometry, Pierini & Möller (2003) have tried to quantify the effects of optical heating and disk opacity on the derivation of SFR from FIR luminosities. For this they investigated trends in the ratio of the far-IR luminosity to the intrinsic UV luminosity, L_{dust}/L_{UV}, with both disk opacity and disk mass (as measured by the intrinsic K-band luminosity). Using a separate relation between disk opacity and K band luminosity they were able re-express L_{dust}/L_{UV} in terms of a single variable, the galaxy mass In this way they found evidence for the relative importance of optical photons in heating dust to increase with increasing galaxy mass.

In the MIR, the correlation of global MIR and Hα luminosities is also non-linear (Roussel et al., 2001a), but since the MIR SED is so constant from galaxy to galaxy, an explanation along the lines developed for the FIR correlation is not possible. However, Roussel et al. (2001a) have shown that the non-linearity is due again to the fact that the global MIR flux mixes together the contributions from the central regions and the disk. Restricting their studies to the disk emission, they showed that both the 6.75 μm and the 15 μm luminosities are linearly correlated with the extinction-corrected Hα luminosities (see Fig. 11). Therefore, although the MIR emission from the disk of spiral galaxies does not originate directly in the star-forming regions, but rather from the PDRs around them, it is the energy from the star-formation process that powers the MIR luminosity, and Roussel et al. provide the conversion factors that allow the derivation of the star-formation rate (SFR) from the MIR luminosities. In a follow-up study, Förster-Schreiber et al. (2004) demonstrated that the 6.75 μm luminosity is still as good a tracer of star-formation in the central regions of spiral galaxies as it was in their disks. The non-linearity observed in the global 6.75-Hα diagram is attributed to the difference in extinction between disk and central star-forming regions. For the 15 μm luminosities, Förster-Schreiber et al. (2004) showed that the star-formation activity observed in the central regions of galaxies is such that it shifts the emission from very small grains (usually emitting in the 20-60 μm range) toward shorter wavelengths. Therefore, even when the Hα emission is corrected for the higher central extinction, the correlation with the 15 μm emission is not linear as grains that make the IR emission change their thermal regime.

2.3. Quantitative interpretation of FIR SEDs

When considered in isolation, the FIR luminosity of normal galaxies is a poor estimator of the SFR. There are two reasons for this. Firstly, these systems are only partially opaque to the UV light from young stars, exhibiting large variations in the escape probability of UV photons between different galaxies. Secondly, the optical luminosity from old stellar populations can be so large in comparison with the UV luminosity of young stellar populations that a significant fraction of the FIR luminosity can be powered by optical photons, despite the higher probability of absorption of UV photons compared to optical photons.

One step towards a quantitative interpretation of FIR SEDs was achieved by the semi-empirical models of Dale et al. (2001) and Dale & Helou (2002). These authors have used ISO observations to develop
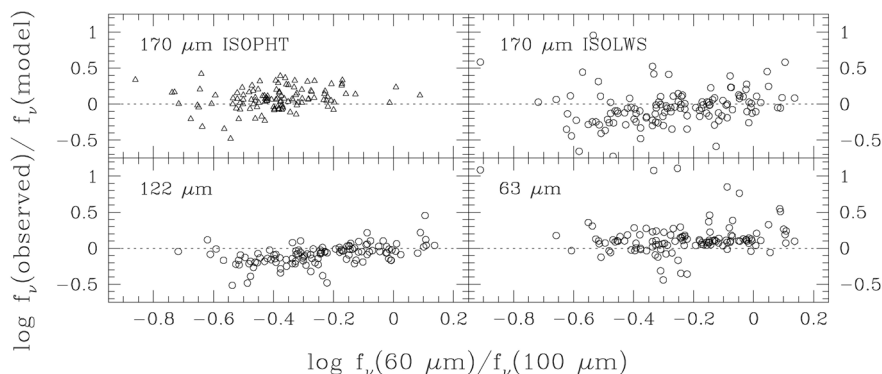
Figure 12. Comparison of observed FIR continuum levels observed by ISO with the model predictions of Dale & Helou (2002). The circles derive from the ISO LWS templates and the triangles represent $170\,\mu m$ data from the ISOPHOT Serendipity Survey (Stickel et al. 2000).

a family of templates to fit the variety of the observed forms of the IR SEDs. This work assumes a power law distribution of dust masses with local radiation field intensity to provide a wide range of dust temperatures. It appears to indicate that the SEDs of star-forming galaxies can be fitted by a one-parameter family of curves (characterised by the $60/100\,\mu m$ colour), determined essentially by the exponent, α, of the power law distribution of dust masses with the radiation field intensity, where the radiation field is assumed to have the colour of the local ISRF. This calibration method has been extensively used to predict FIR flux densities longwards of $100\,\mu m$ for the galaxies not observed by ISOPHOT. A comparison of the FIR continuum levels observed by ISO with the Dale & Helou (2002) model predictions is shown in Fig. 12. However, a quantitative interpretation of dust emission in terms of SFRs and star-formation histories requires a combined analysis of the UV-optical/FIR-submm SEDs, embracing a self-consistent model for the propagation of the photons.

There are a few such models in use which incorporate various geometries for the stellar populations and dust (Silva et al. 1998, Bianchi et al. 2000a, Charlot & Fall 2000, Popescu et al. (2000b)). We will concentrate here on the model of Popescu et al., since this is the only model which has been used to make direct predictions for the spatial distribution of the FIR emission for comparison with the ISO images. This model also ensures that the geometry of the dust and stellar populations is consistent with optical images. Full details are given by Popescu et al. (2000b), Misiriotis et al. (2001), Popescu & Tuffs (2002b) and Tuffs et al. (2004). In brief, the model includes solving the
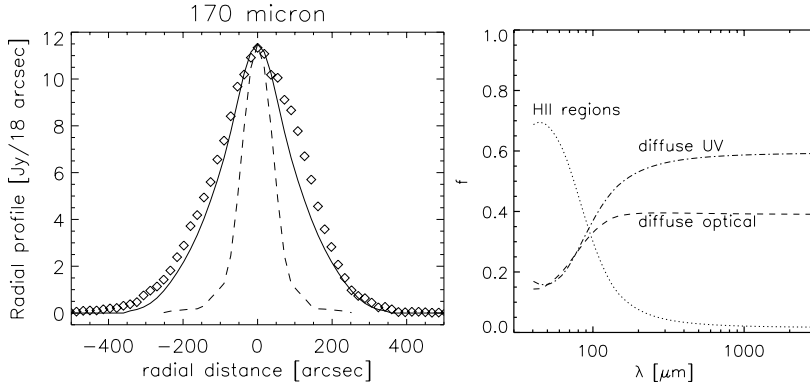
Figure 13. Left: The radial profile of NGC 891 at $170\,\mu$m (Popescu et al. 2004) produced by integrated the emission parallel to the minor axis of the galaxy for each bin along the major axis. Solid line: model prediction; diamonds: observed profile; dotted line: beam profile. Right: The fractional contribution of the three stellar components to the FIR emission of NGC 891 (Popescu et al. 2000b).

radiative-transfer problem for a realistic distribution of absorbers and emitters, considering realistic models for dust, taking into account the grain-size distribution and stochastic heating of small grains and the contribution of HII regions. The FIR-submm SED is fully determined by just three parameters: the star-formation rate SFR, the dust mass M_{dust} associated with the young stellar population, and a factor F, defined as the fraction of non-ionising UV photons which are locally absorbed in HII regions around the massive stars. A self-consistent theoretical approach to the calculation of the F factor is given by Dopita et al. (2005) in the context of modelling SEDs of starburst galaxies.

Popescu et al. (2000b) illustrated their model with the example of the edge-on galaxy NGC 891, which has been extensively observed at all wavelengths (including the complete submm range; Dupac et al. 2003), and also mapped with ISOPHOT at 170 and $200\,\mu$m (Popescu et al. 2004). A particularly stringent test of the model was to compare its prediction for the radial profile of the diffuse dust emission component near the peak of the FIR SED with the observed radial profiles. This comparison (see Fig. 13, left panel) done in Popescu et al. (2004) showed a remarkable agreement. The excess emission in the observed profile with respect to the predicted one for the diffuse emission was explained in terms of two localised sources.

At 170 and $200\,\mu$m the model for NGC 891 predicts that the bulk of the FIR dust emission is from the diffuse component. The close agreement between the data and the model predictions, both in integrated flux densities, but especially in terms of the spatial distribution,

constitutes a strong evidence that the large-scale distribution of stellar emissivity and dust predicted by the model is in fact a good representation of NGC 891. In turn, this supports the prediction of the model that the dust emission in NGC 891 is predominantly powered by UV photons.

Depending on the FIR/submm wavelength, the UV-powered dust emission arises in different proportions from within the localised component (HII regions) and from the diffuse component (Fig. 13; right panel). For example at $60\,\mu$m, 61% of the FIR emission in NGC 891 was predicted to be powered by UV photons locally absorbed in star-forming complexes, 19% by diffuse UV photons in the weak radiation fields in the outer disk (where stochastic emission predominates), and 20% by diffuse optical photons in high energy densities in the inner part of the disk and bulge. At $100\,\mu$m the prediction was that there are approximately equal contributions from the diffuse UV, diffuse optical and locally absorbed UV photons. At 170, $200\,\mu$m and submm wavelengths, most of the dust emission in NGC 891 was predicted to be powered by the diffuse UV photons. The analysis described above does not support the preconception that the weakly heated cold dust (including the dust emitting near the peak of the SED sampled by the ISOPHOT measurements presented here) should be predominantly powered by optical rather than UV photons. The reason is as follows: the coldest grains are those which are in weaker radiation fields, either in the outer optically thin regions of the disk, or because they are shielded from radiation by optical depth effects. In the first situation the absorption probabilities of photons are controlled by the optical properties of the grains, so the UV photons will dominate the heating. The second situation arises for dust associated with the young stellar population, where the UV emissivity far exceeds the optical emissivity.

2.4. THE GASEOUS ISM

2.4.1. *The atomic component*
Most ISO studies of the ISM in normal galaxies focussed on observations with LWS of the [C II] $158\,\mu$m fine structure transition, which is the main channel for cooling of the diffuse ISM. Prior to ISO, knowledge of [C II] emission from external galaxies was limited to measurements of a total of 20 strongly star-forming galaxies sufficiently bright to be accessible to the Kuiper Airborne Observatory (Crawford et al. 1985; Stacey et al. 1991; Madden et al. 1993). The main conclusion of these early investigations was that the [C II] line emission arose from PDRs, where the UV light from young stars impinged on molecular clouds in star-forming regions. The only exception to this was Madden et al's

resolved study of NGC 6946, who showed that the line could also be emitted from the diffuse disk.

The principal contributions of ISO to the knowledge of the neutral gaseous ISM have been twofold: Firstly, knowledge of the [C II] line emission has been extended to quiescent spiral galaxies and dwarf galaxies. These targets are difficult to access from beneath the atmosphere on account of their low luminosities and brightnesses. Secondly, ISO has tripled the number of higher luminosity systems with [C II] measurements, and has also observed a whole range of other fine structure lines in these systems. These lines have been used to probe in detail the identity of the emitting regions and their physical parameters.

Fundamental to the studies of the quiescent spiral galaxies were the measurements by Leech et al. (1999), who detected 14 out of a sample of 19 Virgo cluster spirals (a subset of the IVCDS sample - see Sect. 2.2) in the [C II] line using LWS. These galaxies are the faintest normal galaxies ever measured in the [C II] line, and can be regarded as quiescent in star-forming activity ($H\alpha$ EW is less than 10 Å for 8 galaxies). In a series of papers Pierini & collaborators (Pierini et al. 1999; Pierini et al. 2001, & Pierini et al., 2003a) used these LWS data, in combination with the existing KAO measurements of more actively star-forming galaxies, to investigate the physical origin of the line emission in normal galaxies as a function of star-formation activity. The main result was that the [C II] emission of quiescent systems predominantly arises from the diffuse ISM (mainly the cold neutral medium; CNM), as evidenced from the fact that these systems occupy a space in the $L_{[C\ II]}/L_{CO}$ versus $L_{[C\ II]}/L_{FIR}$ diagram devoid of individual star-formation regions or giant molecular clouds (Pierini et al. 1999). An origin of the [C II] emission from the CNM had earlier been proposed by Lord et al. (1996) as an alternative to an origin in localised PDRs, on the basis of a full LWS grating spectrum of the spiral galaxy NGC 5713.

The luminosity ratio of [C II] line emission to FIR dust emission, $L_{[C\ II]}/L_{FIR}$, was found to be in the range 0.1 to 0.8% for the quiescent spirals. This is consistent with the basic physical interpretation, originally established for the more active galaxies, of a balance between gas cooling (mainly through the [C II] line) and gas heating through photoelectric heating from grains[1] However, the range of a factor of almost an order of magnitude in the observed values of $L_{[C\ II]}/L_{FIR}$ also suggests that the relation between the [C II] line emission and the

---

[1] The exception is the Virgo cluster galaxy NGC 4522, which was found by Pierini et al. (1999) to have an abnormally high value for $L_{[C\ II]}/L_{FIR}$, possibly indicating mechanical heating of the interstellar gas as the galaxy interacts with the intracluster medium.
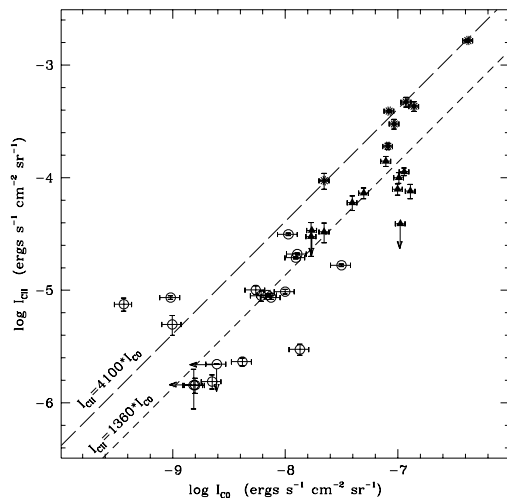
Figure 14. The relationship between the observed central [CII] line intensity, $I_{[CII]}$, and the central CO line intensity, I_{CO} from Pierini et al. (2001). Asterisks and filled triangles denote starburst galaxies and gas-rich galaxies of the KAO sample, while open circles identify spiral galaxies of the ISO sample. The long- and short-dashed lines show the average ratios of the two observables obtained by Stacey et al. (1991) for the starburst galaxies and the gas-rich galaxies, respectively.

SFR may be quite complex. This impression is reinforced by the large scatter and non-linearities found by Boselli et al. (2002) in the relations between the [C II] luminosity and SFRs derived from Hα measurements for a sample principally composed of the Virgo galaxies measured by Leech et al. (1999) with the LWS.

One consequence of the physical association of the [C II] emission with the diffuse dusty ISM in quiescent galaxies is that the observed $L_{[C\ II]}/L_{FIR}$ ratio will be reduced due to an optically- (rather than UV-) heated component of the FIR dust emission. A model quantifying this effect was developed by Pierini et al. (2003a) in which $L_{[C\ II]}/L_{FIR}$ depends on the fractional amount of the non-ionising UV light in the interstellar radiation field in normal galaxies. Overall, systematic variations in the $L_{[C\ II]}/L_{FIR}$ ratio for star-forming galaxies can be summarised as follows: In progressing from low to high star-formation activities, $L_{[C\ II]}/L_{FIR}$ first increases in systems in which the [C II] emission is mainly from the diffuse medium, due to a decrease in importance of optical photons in heating the diffuse dust. After reaching a maximum, $L_{[C\ II]}/L_{FIR}$ then decreases as the star-formation

activity is further increased to starburst levels, due to an increase in the fraction of [C II] emission arising from localised PDRs associated with star-forming regions, coupled with the quenching of the [C II] emission through the decreased efficiency of photoelectric heating of the gas in high radiation fields. Thus, the dominance of the [CII] emission from PDRs turned out to be the asymptotic limit for high SFR in gas-rich galaxies.

The LWS observations of Virgo spirals also showed that the linear relation between $L_{[C\ II]}$ and L_{CO} previously established for starburst systems extends into the domain of the quiescent spirals, though with an increased scatter (see Fig. 14). The tight relation between $L_{[C\ II]}/L_{CO}$ and the Hα equivalent width (EW) found by Pierini et al. (1999) indicated that this scatter may be induced by different strengths of the far-UV radiation field in galaxies. Alternatively, as discussed by Smith & Madden (1997) in their study of five Virgo spirals, the fluctuations in $L_{[C\ II]}/L_{CO}$ from one galaxy to the next might reflect changes in L_{CO} from PDRs caused by variations in metallicity (and dust abundance), as well as varying fractions of [C II] emission arising from PDRs and the cold neutral medium. The measurements of the [C II]/CO line ratios derived from ISO observations have also thrown new light on the much debated relation between the strength of the CO line emission and the mass of molecular hydrogen in galaxies. Bergvall et al. (2000) emphasise how the low metallicity, the intense radiation field and the low column density in the dwarf starburst galaxy Haro 11 can explain the extremely high observed [C II]/CO flux ratio, indicating that CO may be a poor indicator of the H_2 mass in such systems. Similarly, the enhanced [C II]/CO ratios found in the Virgo spirals observed by Smith & Madden (1997) were attributed to the low metallicities in these galaxies, although, as also pointed out by these authors, an alternative explanation could be that radiation from diffuse HI may dominate the [C II] emission.

Mapping observations of the [C II] line using the LWS provide a means to directly probe the relative amounts of [C II] arising from localised PDRs associated with star-forming regions in the spiral arms and the diffuse disk, as well to investigate the relation between the [C II] emission and the neutral and molecular components of the gas. They have also allowed the nuclear emission to be separately studied. Contursi et al. (2002) mapped the two nearby late-type galaxies NGC 1313 and NGC 6946 in the [C II] line, finding that the diffuse HI disk contributes $\leq\sim40$ % and ~30 % of the integrated [C II] emission in NGC 6946 and NGC 1313, respectively. CO(1-0) and [C II] were also found to be well correlated in the spiral arms in NGC 6946, but less well so in NGC 1313. Stacey et al. (1999) mapped the barred spiral

M83 in a variety of fine structure lines in addition to the [C II] line - the [O I] 63 & 145 μm lines, the [N II] 122 μm line and the [O III] 88 μm line, and obtained a full grating scan of the nucleus. At the nucleus, the line ratios indicate a strong starburst headed by O9 stars. Substantial [N II] emission from low density HII regions was found in addition to the anticipated component from PDRs. A further resolved galaxy studied with the LWS is M33, for which Higdon et al. (2003) made measurements of fine structure lines and dust continuum emission towards the nucleus and six giant HII regions. Overall, the picture presented by these investigations of resolved galaxies is broadly in accordance with the theory that the integrated [C II] emission from spirals galaxies is comprised of the sum of components from the diffuse disk and from localised PDRs and diffuse ionised gas associated with star-formation regions in the spiral arms.

Fundamental to the statistical investigations of gas in more active galaxies are the full grating spectra of 60 normal galaxies from the ISO key-project sample of Helou et al. (1996), which were obtained by Malhotra et al. (1997, 2001) with the LWS. One of the main results was the discovery of a smooth but drastic decline in $L_{[C\ II]}/L_{FIR}$ as a function of increasing star-formation activity (as traced by the L_{60}/L_{100} IRAS colour ratio or L_{FIR}/L_B) for the most luminous third of the sample. This trend was accompanied by a increase in the ratio of the luminosity of the [O I] 63 μm line to that of the [C II] line. This is readily explained in PDR models in terms of a decreased efficiency of photoelectric heating of the gas as the intensity of the UV radiation field is increased, coupled with an increased importance of the [O I] cooling line as the gas temperature is increased. Both Malhotra et al. (2001) and Negishi et al. (2001) present a comprehensive analysis of the ratios of the most prominent lines ([C II] 158 μm; [O I] 63 & 145 μm; [N II] 122 μm; [O III] 52 & 88 μm and [N III] 57 μm) in terms of the densities of gas and radiation fields in PDRs, as well as of the fraction of emission that comes from the diffuse ionised medium (as traced by [N II] 122 μm). Malhotra et al (2001) found that the radiation intensities G_0 increases with density n as $G_0 \propto n^\alpha$, with α being ~ 1.4. They interpret this result, together with the high PDR temperatures and pressures needed to fit the data, as being consistent with the hypothesis that most of the line and continuum luminosity of relatively active galaxies arises from the immediate proximity of the star-forming regions. By contrast, on the basis of a comparison of the [C II] line with the [N II] 122 μm line, Negishi et al. (2001) argue that a substantial amount (of order 50%) of the [C II] line emission might arise not from PDRs but instead from low density diffuse ionised gas. Negishi et al. (2001) also found a linear (rather than non-linear) relation between G_0 and n, which would argue

against a decreased photoelectric heating efficiency being responsible for the decline in $L_{[C\ II]}/L_{FIR}$ with star-formation activity. Instead, Negishi et al. invoke either an increase in the collisional de-excitation of the line with increasing density, or a decrease in the diffuse ionised component with increasing star-formation activity as being responsible for this effect.

An explanation for the decrease in $L_{[C\ II]}/L_{FIR}$ in terms of a decreased efficiency of photoelectric heating of the gas (Malhotra et al. 2001) or due to a collisional de-excitation of the [C II] line (Negishi et al. 2001) would predict that the $L_{[C\ II]}$ will not be a good probe of high redshift starburst galaxies. However, an alternative (or complementary) explanation for the decrease in $L_{[C\ II]}/L_{FIR}$ with star-formation activity, proposed by Bergvall et al. (2000), is that the line becomes self-absorbed in local universe starbursts with high metallicity. This scenario would also explain why the metal poor luminous blue compact dwarf galaxy Haro 11 was found by Bergvall et al. to have a high ratio of $L_{[C\ II]}/L_{FIR}$, despite the intense radiation fields present.

2.4.2. *The molecular component*

The lowest energy transitions of the most abundant molecule in the Universe, H_2, are located in the MIR, typically between 3 and 30 μm. These pure rotational lines potentially offer a new access to the molecular component of the ISM, to be compared with the less direct CO tracer. One caveat though is that the lines can be excited by different mechanisms, typically shocks or UV-pumping, which render their interpretation difficult. Furthermore, the emission is very rapidly dominated by that from the warmest fraction of the gas, and therefore this new tracer offers only a partial and complex access to the molecular phase.

Most of the extragalactic H_2 detections were made with ISOSWS (de Graauw et al., 1996; Leech et al., 2003)), since high spectral resolution is necessary to isolate the very thin molecular lines from the broader features that abound in the MIR regime (although a tentative detection in NGC 7714 made with ISOCAM is presented by O'Halloran et al., 2000). For sensitivity reasons, the galaxies that were observed in these lines tended to be starburst or active galaxies and are discussed elsewhere in this volume.

Nevertheless, the S(0) and S(1) transitions were observed in the central region and in the disk of NGC 6946 (Valentijn et al., 1996 and Valentijn & van der Werf, 1999a) and all along the disk of NGC 891 Valentijn & van der Werf (1999b). In the central region of NGC 6946, the molecular component detected with ISOSWS is clearly the warm fraction (of order 5-10%) of the molecular gas present in the region and is raised to the observed temperature of 170 K by the enhanced

star-formation activity in the center of the galaxy. H_2 is also detected further out (4 kpc) in the disk, with a cooler temperature, though still relatively warm.

The observations of H_2 in the disk of NGC 891 reach much larger distances, extending about 10 kpc on both sides of the nucleus. Valentijn & van der Werf (1999b) argue that the observed line ratios indicate the presence of both warm (150-230 K) molecular gas, identical as that observed in NGC 6946, and cool (80-90 K) molecular gas. This cooler gas needs to have a very large column density to explain the observed surface brightness and the masses derived by Valentijn & van der Werf (1999b) are in fact so large that they would resolve the missing mass problem in the optical disk of NGC 891. This highly controversial conclusion however rests on a rather uncertain basis dealing with the actual spatial distribution of the H_2-emitting clouds within the ISOSWS beam. Upcoming observations with the IRS on Spitzer should remove the remaining uncertainties regarding the presence of large amounts of cold H_2 in the disks of galaxies.

3. Dwarf Galaxies

3.1. Cold dust surrounding dwarf galaxies

Gas-rich dwarf galaxies and in particular Blue Compact Dwarfs (BCDs) were originally expected to have their FIR emission dominated by dust heated locally in HII regions. Temperatures of 30 K or more were anticipated. This was the a priori expectation in particular for the BCDs, and became the standard interpretation for the IRAS results obtained for these systems. Hoffman et al. (1989), Helou et al. (1988) and Melisse & Israel (1994) each found that the $60/100\,\mu$m colours of BCDs were clearly warmer than those of spirals.

The IVCD Survey (Tuffs et al. 2002a,b) changed that simple picture of the FIR emission from dwarf galaxies. The IVCDS included measurements at 60, 100, and (for the first time) at $170\,\mu$m of 25 optically selected gas-rich dwarf galaxies. The observations at 60 and $100\,\mu$m were consistent with the previous IRAS results on this class of galaxies, though extending knowledge of these systems to lower intrinsic luminosities. Unexpectedly however, high ratios of $170/100\,\mu$m luminosities were found in many of the surveyed systems. Such long-wavelength excesses were found both in relatively high-luminosity dwarfs, such as VCC655, as well as in fainter objects near the limiting sensitivity of the survey. These observations imply the presence of large amounts of cold dust.

As shown by Popescu et al. (2002), it seems unlikely that the cold dust resides in the optically thick molecular component associated with star-formation regions, since the implied dust masses would be up to an order of magnitude greater than those typically found in giant spirals. Such large masses could not have been produced through star-formation within the dwarfs over their lifetime. One alternative possibility is that the dust originates and still resides outside the optical extent of these galaxies. In fact, some evidence for this was provided by the ISOPHOT observations themselves, since they were made in the form of scan maps, from which estimates of source sizes could be determined. Even with the relatively coarse beam (1.6′ FWHM at 170 μm), the extended nature of the sources could be clearly seen in a few cases for which the FWHM for the 170 μm emission exceeds the optical diameters of the galaxies (to 25.5Bmag/arcsec^2) by factors of between 1.5 and 3.5. It is interesting to note that two of these galaxies (VCC 848 and VCC 81) have also been mapped in H I (Hoffman et al. 1996), revealing neutral hydrogen sizes comparable to the 170 μm extent. This raises the possibility that the cold dust is embedded in the extended H I gas, external to the optical galaxy. This would be analogous to the case of the edge-on spiral NGC 891, where Popescu & Tuffs (2003) discovered a cold-dust counterpart to the extended H I disk (see Sect. 2.1.3). In this context the main observational difference between the giant spiral and the dwarfs may be that for the dwarfs the integrated 170 μm emission is dominated by the extended emission component external to the main optical body of the galaxy, whereas for the giant spirals the long-wavelength emission predominantly arises from within the confines of the optical disk of the galaxy.

Apart from the SMC (which is discussed in Sect. 3.2 and is too extended for ISOPHOT to map beyond its optical extent), only three dwarf galaxies were observed by ISOPHOT in the field environment (all Serendipity Survey sources; Stickel et al. 2000). All three sources have comparable flux densities at 100 and 170 μm. But the small statistics mean that it is still an open question to which extent the cold dust emission associated with the extended H I component in dwarf galaxies is a cluster phenomenon or not.

The existence of large quantities of dust surrounding gas-rich dwarf galaxies may have important implications for our understanding of the distant Universe. According to the hierarchical galaxy formation scenarios, gas-rich dwarf galaxies should prevail at the earliest epochs. We would then expect these same galaxies to make a higher contribution to the total FIR output in the early Universe, certainly more than previously expected.

3.2. Infrared emission from within dwarf galaxies

The distribution of cold dust within dwarf galaxies could be studied in only one case, namely in the resolved ($1.5'$ resolution) $170\,\mu$m ISOPHOT map of the Small Magellanic Cloud (Wilke et al. 2003, Wilke et al. 2004). The $170\,\mu$m ISO map of the SMC reveals a wealth of structure, not only consisting of filamentary FIR emitting regions, but also of numerous (243 in total) bright sources which trace the bar along its major axis as well as the bridge which connects the SMC to the LMC. Most of the brighter sources have cold components, associated with molecular clouds. The discrete sources were found to contribute 28%, 29% and 36% to the integrated flux densities at 60, 100 and $170\,\mu$m, respectively. The SED was modelled by the superposition of $45\,$K, $20.5\,$K and $10\,$K blackbody components with emissivity index $\beta=2$. The average dust colour temperature (averaged over all pixels of the 170/100 colour map) was found to be $T_\mathrm{D} = 20.3\,$K.

Bot et al. (2004) have compared the FIR map of the SMC with an Hi map of similar resolution. This reveals a good spatial correlation of the two emissions in the diffuse regions of the maps (regions that fall outside of the correlation are either hot star-forming regions, or cold molecular clouds with no associated Hi). Adding the IRAS data allows them to compute the FIR emissivity per unit H atom. Bot et al. (2004) found that this emissivity is lower than in the Milky Way, and in fact it is even lower than the lower metallicity ($Z_\odot/10$) of the SMC would imply, suggesting that depletion mechanisms at work in the ISM have more than a linear dependence on metallicity.

Although FIR emission from dwarf galaxies has been associated only with gas-rich dwarfs, in one particular case such emission has been detected in a dwarf elliptical galaxy, as well. This is the case of NGC 205, one of the companions of M 31, classified as a peculiar dE5. This galaxy shows signatures of recent star-formation (Hodge 1973) and of extended HI emission (Young & Lo 1997), and was detected by IRAS (Rice et al. 1988, Knapp et al. 1989), with a SED steeply rising between 60 and $100\,\mu$m. Based on ISOPHOT observations, Haas (1998) showed that the FIR emission is resolved and similar to that seen in HI. He also presented evidence for a very cold dust component, of 10 K, coming from the center of the galaxy.

The properties of gas-rich dwarf galaxies were found to markedly differ from those of spiral galaxies at shorter IR wavelengths. Thus, when comparing the MIR emission of five IBm galaxies to their Hα or FIR properties, Hunter et al. (2001) discovered a noticeable deficit of the $6.75\,\mu$m component in their galaxies. This deficit is not observed at $15\,\mu$m, i.e. the 6.75/15 μm flux ratio is very different in IBm galaxies
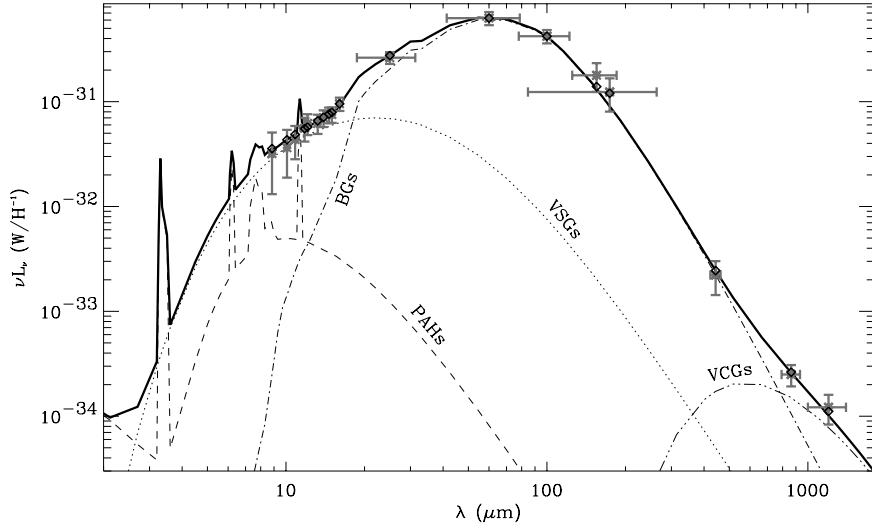
Figure 15. NGC 1569 observations and modeled SED from Galliano et al. (2003). The data are indicated by crosses: vertical bars are the errors on the flux density values and the horizontal bars indicate the widths of the broadbands. The lines show the predictions of the dust model with its different components. Diamonds indicate the model predictions integrated over the observational broadbands and colour-corrected.

than in spirals, which is interpreted as tracing both a deficit of PAH, possibly destroyed by the radiation field, and an increase of the mean temperature of the very small grains, again linked to the radiation field (see also O'Halloran et al., 2000). This interpretation of the observations is confirmed by detailed spectroscopic measurements of similar objects. In NGC 5253 the MIR SED is dominated by a "hot" continuum from which the PAH features are absent (Crowther et al., 1999). The blue compact galaxy II Zw 40 presents a similar spectrum, i.e. a strongly rising continuum with no bands (Madden, 2000). In both cases this is interpreted as being the result of very hard radiation fields that both destroy the PAH and shift the continuum emission from very small grains toward shorter wavelengths. These galaxies are essentially small starburst regions and their IR spectrum thus reflects the IR properties of starburst galaxies discussed elsewhere in this volume. That we are indeed seeing a gradual destruction of PAHs, and not an effect of metallicity that would prevent the formation of these species is demonstrated by the fact that we find galaxies of similar metallicity (NGC 5253 and NGC 1569 for instance at $Z_\odot/4 - Z_\odot/5$) without or with PAH emission (see Galliano et al., 2003 for NGC 1569). In fact, even the SMC at

$Z_\odot/10$ has a MIR spectrum with pronounced PAH features (Reach et al., 2000).

Many of the qualitative indications about grain and PAH abundance indicated above have been quantitatively estimated by Galliano et al. (2003) in their detailed modelling of the UV-optical/MIR-FIR-submm SED of the low metallicity nearby dwarf galaxy NGC1569. (Fig. 15). This study is noteworthy in that it constrains the grain size distribution through the MIR-FIR ISOCAM and ISOPHOT observations and therefore gives more specific information about grain properties in dwarf galaxies. The results confirm the paucity of PAHs due to an enhanced destruction in the intense ambient UV radiation field, as well as an overabundance (compared to Milky Way type dust) of small grains of size $\sim 3\,\mathrm{nm}$, possibly indicative of a redistribution of grain sizes through the effect of shocks.

4. Early-type galaxies

Here we use the term "early-type" to embrace both elliptical and lenticular galaxies. Their IR emission, when detected, has been interpreted very differently from the IR emission from spiral galaxies. Indeed, early-type galaxies belong to a subset of the Hubble sequence where star-formation activity is at its minimum, or has stopped, and the ISM is almost exhausted. Given what we have seen above, one does not expect these objects to be IR bright. This is indeed the case, judging from the small fraction of early-type objects in the IRAS catalogues (see e.g. Jura et al., 1987), and the large uncertainties associated with their fluxes (Bregman et al., 1998). For those few galaxies where IR emission is detected, it is commonly attributed either to the Rayleigh-Jeans tail of the stellar emission, or to dust in mass-losing stars. These interpretations however rest on the 4 broad-band low spatial resolution data of IRAS. ISO, with its much improved sensitivity to both spatial and spectral details, has shone a sharper light on the subject.

The FIR observations of early-type galaxies selected from the ISO archive have been analysed by Temi et al. (2004). They found that the FIR SED requires emission from dust with at least two different temperatures, with mean temperatures for the warm and cold components of 43 and 20 K, respectively. This result is quite similar to the results obtained for quiescent spiral galaxies, in particular to the result obtained by Popescu et al. (2002) for the Virgo Cluster spiral galaxies. Since ellipticals are known to be ISM-poor and have reduced star-formation activity, the similarity between their FIR properties and those of spirals is surprising. One explanation could be the fact that the

galaxies included in the ISO archive are not representative of typical ellipticals. As pointed out by Temi et al., many galaxies selected for ISO observations were chosen because they were known to have large IRAS fluxes or large masses of cold gas, and in this sense they have properties closer to those of spirals. For the same reason Temi et al. considered that these IR-selected galaxies are likely to have experienced unusual dust-rich mergers, and that the dust in these galaxies could have an external origin. The lack of a correlation found between the FIR luminosity (or dust mass) and the luminosity of the B band emission was taken as evidence for this scenario. Another scenario proposed is one in which most of the FIR is emitted by central dust clouds, where the clouds could be disturbed at irregular intervals by low-level AGN activity in the galactic cores, creating the stochastic variation in the FIR luminosity. It is difficult to distinguish between these two scenarios, also because the sensitivity of ISO was not sufficient to detect FIR emission from many optically luminous elliptical galaxies. In order to distinguish between an external and an internal origin for the dust, deeper FIR observations of an optically selected sample of elliptical galaxies are needed. It is even possible that such surveys may occasionally detect bright FIR emission from galaxies traditionally classified as ellipticals, but which in fact have hidden starburst activity in their central regions. This is the case for the IRAS source F15080+7259, which was detected in the ISOPHOT serendipity survey, and was shown by Krause et al. (2003) to harbour large quantities of gas and cold dust.

Another elliptical detected by ISOPHOT is the Virgo Cluster galaxy M 86 (NGC 4406). The deep FIR imaging data obtained with ISOPHOT at 60, 90, 150 and 180 μm revealed a complex FIR morphology for this galaxy (Stickel et al. 2003). It was found that the FIR emission originates from both the centre of M 86 and from the optically discovered dust streamers, and has a dust temperature of 18 K. Again, this elliptical is not representative for this class of objects, since it was considered either to be experiencing ram-pressure stripping or to be gravitationally interacting with its neighbouring galaxies. In particular the ISOPHOT observations were interpreted by Stickel et al. as being consistent with M 86 having a gravitational interaction with its nearest spiral galaxy NGC 4402. In this case the detected dust would again have (at least in part) an external origin. The importance of gravitational interaction as a driver for FIR emission in early-type galaxies was demonstrated by Domingue et al. (2003), who showed these systems to have a 50% detection rate with ISOPHOT when they are paired with spirals.

In the MIR ISOCAM was used to observe both elliptical and lenticular galaxies, though the objects selected differ from those observed by ISOPHOT. An unbiased sample of 16 IRAS-detected lenticular galaxies

was observed using low resolution MIR spectroscopy by Sauvage et al. (2004). The vast majority of the detected galaxies present MIR SEDs extremely similar to those of later-type spiral galaxies (i.e. PAH bands). Thus, from their MIR spectral properties, lenticular galaxies appear to belong to the spiral galaxy group, although with smaller luminosities.

Elliptical galaxies have drawn much more interest from ISOCAM observers, even though they are ISM-poorer than the lenticulars. The main result from these studies is that elliptical galaxies are really a mixed bag, as far as their MIR properties are concerned. Quillen et al. (1999) mapped with ISOCAM a number of E+A galaxies[2] in the Coma cluster, but detected only those which showed emission lines characteristic of an on-going star-formation episode. This might be thought to imply that star-formation is required for ellipticals to emit in the MIR, but in fact more likely reflects the sensitivity reached by Quillen et al.. With deep ISOCAM observations of closer "normal" elliptical galaxies, Athey et al. (2002) showed that their MIR emission is dominated by the emission from K and M stars, with the addition of a spectral feature near $10\,\mu$m that they attribute to silicates in the circumstellar envelopes of AGB stars. Xilouris et al. (2004) brought balance to the star/ISM debate for the origin of MIR emission in early-type galaxies by showing that the complete range of phenomena occur in this class of galaxies. Systems vary from those that are dominated up to $\sim 20\,\mu$m by the emission from their old stellar populations to those in which a small star-forming episode, possibly fueled by recent accretion, dominates the MIR luminosities. In between one also finds galaxies where only the long-wavelength part of the MIR spectrum deviates from the extrapolation of the stellar light, which indicates the presence of small amounts of diffuse dust much hotter than what is commonly found in spirals. This is most likely to be due to the higher interstellar radiation field generated by the denser stellar populations.

Although ISO has had some success in detecting and measuring the IR SED from early-type galaxies, a critical look at the observations done reveals that we still do not know the IR properties of typical elliptical galaxies. To achieve this, systematic deep observations of optically selected samples are required.

5. Conclusions and Outlook

ISO has not only advanced the knowledge of IR properties of normal galaxies but has also made unexpected discoveries. The bulk of the

---

[2] Early-type galaxies showing evidence of a post-starburst population.

emission from dust has been measured, revealing cold dust in copious quantities. This dust is present in all types of normal galaxies and is predominantly distributed in a diffuse disk with an intrinsic scalelength exceeding that of the stars. Cold dust has been found beyond the optical regions of isolated galaxies, associated with the extended HI disks of spiral galaxies or with the HI envelopes of dwarf galaxies. The fraction of the bolometric luminosity radiated by dust has been measured for the first time. Realistic geometries for stars and dust have been derived from ISO imaging observations, enabling the contribution of the various stellar populations to the dust heating to be accurately derived. The NIR/MIR SEDs were shown to be remarkably similar for normal spiral galaxies and to originate mostly in the PDRs surrounding star-forming regions. A diffuse component of the MIR emission was found, though puzzlingly with a much smaller scalelength than its FIR counterpart. The importance of the central regions in shaping up the intensity and the colour of the MIR global emission was revealed thanks to the high spatial resolution offered by ISO. A new component of interstellar dust emission consisting of a "hot" NIR continuum emission was discovered. The relative contribution of photospheric and very small grains/ PAH emission has been established in the NIR/MIR spectral region. Spectroscopic observations have revealed that the main interstellar cooling line, [CII], is predominantly carried by the diffuse cold neutral medium in normal galaxies, with emission from localised PDRs only dominating for galaxies having high star-formation activity.

This enormous advancement in the understanding of normal galaxies in the nearby Universe has laid the foundation for more detailed investigations with Spitzer and Herschel. A clear priority is to fill the gap left by ISO in knowledge of the SEDs of normal galaxies between 20-60 μm. Another priority is to increase the number of galaxies with detailed imaging information and to provide better statistics on carefully selected samples, especially those selected in the optical/NIR bands. Ultimately, the improved sensitivity of the new infrared space observatories will allow knowledge of the dust emission from normal galaxies to be extended beyond the nearby universe.

Acknowledgements

Popescu would also like to thank Heinrich J. Völk for enlightening discussions.

References

Alton, P.B., Trewhella, M., Davies, J.I., Evans, R., Bianchi, S., et al. 1998, A&A, 335, 807

Athey, A., Bregman, J., Bregman, J., Temi, P., Sauvage, M. 2002, ApJ 571, 272

Bendo, G.J., Joseph, R.D., Wells, M., Gallais, P., Haas, M. et al. 2002a, AJ 123, 3067

Bendo, G.J., Joseph, R.D., Wells, M., Gallais, P., Haas, M. et al. 2002b, AJ 124, 1380

Bendo, G.J., Joseph, R.D., Wells, M., Gallais, P., Haas, M. et al. 2003, AJ 125, 2361

Bergvall, N., Masegosa, J., Östlin, G, & Cericharo, J., 2000, A&A, 359, 41

Bianchi, S., Davies, J. I., Alton, P. B. 2000a, A&A 359, 65

Bianchi, S., Davies, J. I., Alton, P. B., Gerin, M., & Casoli, F. 2000b, A&A 353, L13

Binggeli, B., Popescu, C.C. & Tammann, G.A. 1993, A&AS, 98, 275

Binggeli, B., Sandage, A. & Tammann, G.A. 1985, AJ, 90, 1681

Blommaert, J., Siebenmorgen, R., Coulais, A. et al. 2003, 'The ISO Handbook, Volume II: CAM - The ISO Camera', ESA SP–1262

Bot, C., Boulanger, F., Lagache, G., Cambrésy, L., Egret, D. 2004 A&A 423, 567

Boselli, A., Gavazzi, G., Lequeux, J. Pierini, D. 2002, A&A 385, 454

Boselli, A., Gavazzi, G., Sanvito, G. 2003a, A&A 402, 37

Boselli, A., Lequeux, J., Contursi, A. Gavazzi, G., Boulade, O., et al. 1997, A&A, 324, L13

Boselli, A., Sauvage, M., Lequeux, J., Donati, A, & Gavazzi, G. 2003b, A&A 406, 867

Bregman, J. N., Snider, B. A., Grego, L., Cox, C. V. 1998, ApJ 499, 670

Cesarsky, C.J. et al. 1996, A&A 315, L32

Cesarsky, D., Lequeux, J., Pagani, L., Ryter, C., Loinard, L., Sauvage, M. 1998, A&A 337, L35

Charlot, S., & Fall, S.M. 2000, ApJ 539, 718

Clegg, P.E. et al. 1996, A&A 315, L38

Contursi, A., Kaufman, M. J., Helou, G. et al. 2002, AJ 124, 751

Contursi, A., Boselli, A., Gavazzi, G., Bertagna, E., Tuffs, R., Lequeux, J. 2001, A&A 365, 11

Contursi, A., Lequeux, J., Hanus, M., Heydari-Malayeri, M., Bonoli, C., Bosma, A., et al. 1998, A&A 336, 662

Contursi, A., Lequeux, J., Cesarsky, D., Boulanger, F., Rubio, M., Hanus, M. et al. 2000, A&A 362, 310

Crawford, M.K., Genzel, R., Townes, C.H., & Watson, D.M. 1985, ApJ 291, 755

Crowther, P. A., Beck, S. C., Willis, A. J., Conti, P. S., Morris, P. W., Sutherland, R. S. 1999, MNRAS 304, 654

Dale, D. & Helou, G. 2002, ApJ 576, 159

Dale, D. A., Helou, G., Contursi, A., Silbermann, N. A. & Kolhatkar, S. 2001, ApJ, 549, 215

Dale, D. A., Helou, G., Silbermann, N. A., Contursi, A., Malhotra, S., Rubin, R. H. 1999, AJ 118, 2055

Dale, D. A., Silbermann, N. A., Helou, G., Valjavec, E., Malhotra, S., Beichmann, C. A., et al. 2000, AJ 120, 583

Davies, J. I., Alton, P., Bianchi, S. & Trewhella, M. 1998, MNRAS 300, 1006

Davies, J.I., Alton, P., Trewhella, M., Evans, R., & Bianchi, S. 1999, MNRAS, 304, 495

de Graauw, T. et al. 1996, A&A 315, L49

de Jong, T., Clegg, P.E., Soifer, B.T.., et al. 1984, ApJ, 278, L67

de Jong, T., Klein, U., Wielebinski, R., Wunderlich, E. 1985, A&A, 147, L6

Domingue, D. L., Sulentic, J. W., Xu, C., Mazzarella, J., Gao, Y., Rampazzo, R. 2003, aj 125, 555

Dopita, M.A., Groves, B.A., Fischera, J., Sutherland, R.S., Tuffs, R.J. et al. 2005, ApJ, in press

Dupac, X., del Burgo, C., Bernard, J.-P., et al. 2003, MNRAS 344, 105

Ferguson, A., Gallagher, J.S. & Wyse, R. 1998, AJ 116, 673

Ferrara, A., Ferrini, F., Barsella, B., & Franco, J. 1991, ApJ 381, 137

Förster-Schreiber, N., Roussel, H., Sauvage, M., Charmandaris, V. 2004, A&A 419, 501

Förster-Schreiber, N., Sauvage, M., Charmandaris, V., Laurent, O., Gallais, P., Mirabel, I. F., et al. 2003, A&A 399, 833

Galliano, F., Madden, S.C., Jones, A.P., Wilson, C.D., Bernard, J.-P., et al. 2003, A&A 407, 159

Gerhard, O. & Silk, J. 1996, ApJ 472, 34

Gry, C., Swinyard, B., Harwood, A. et al. 2003, 'The ISO Handbook, Volume III: LWS - The Long Wavelength Spectrometer', ESA SP–1262

Haas, M. 1998, A&A 337, L1

Haas, M., Klaas, U., Bianchi, S. 2002, A&A 385, L23

Haas, M., Lemke, D., Stickel, M., Hippelein, H., Kunkel, M. et al. 1998, A&A, 338, L33

Helou, G. 1986, ApJ 311, 33

Helou, G., Khan, I. R., Malek, L., & Boehmer, L. 1988, ApJS, 68, 151

Helou, G., Malhotra, S., Beichman, C. A., Dinerstein, H., Hollenbach, D. J., Hunter, D. A., et al. 1996, A&A 315, L157

Helou, G., Malhotra, S., Hollenbach, D. J., Dale, D. A., Contursi, A. 2001, ApJ 548, L73

Helou, G., Roussel, H., Appleton, P., Frayer, D., Stolovy, S., et al. 2004, ApJS, in press

Helou, G., Soifer, B. T., & Rowan-Robinson, M. R. 1985, ApJ, 298, L7

Higdon, S.J.U., Higdon, J.L., van der Hulst, J.M., & Stacey, G.J., 2003, ApJ 592, 161

Hippelein, H., Haas, M., Tuffs, R.J., Lemke, D., Stickel, M. et al. 2003, A&A 407, 137

Hoffman, G. L., Helou, G., Salpeter, E. E., Lewis, B. M. 1989, ApJ, 339, 812

Hodge, P. 1973, ApJ 182, 671

Hoffman, G. L., Salpeter, E. E., Farhat, B., Roos, T., Williams, H., and Helou, G. 1996, ApJS 105, 269

Hunter, D. A., Kaufman, M., Hollenbach, D. J., Rubin, R. H., Malhotra, S., et al. 2001, ApJ 553, 121

Jura, M., Kim, D. W., Knapp, G. R., Guhathakurta, P. 1987, ApJ 312

Knapp, G.R., Guhathakurta, P., Kin, D.W., Jura, M. 1989, ApJS 70, 329

Kessler, M.F. et al. 1996, A&A 315, L27

Kessler, M.F., Mller, T.G., Leech, K. et al. 2003, 'The ISO Handbook, Volume I: ISO - Mission & Satellite Overview', ESA SP–1262

Kraemer, K. E., Price, S. D., Mizuno, D. R., Carey, S. J. 2002, AJ 124, 2990

Krause, O., Lisenfeld, U., Lemke, D. et al. 2003, A&A 402, L1

Krügel, E., Siebenmorgen, R., Zota, V., Chini, R. 1998, A&A, 331, L9

Laureijs, R.J., Klaas, U., Richards, P.J. et al. 2003, 'The ISO Handbook, Volume IV: PHT - The Imaging Photo-Polarimeter', ESA SP–1262

Leech, K.J., Völk, H.J., Heinrichsen, I., Hippelein, H., Metcalfe, L., et al. 1999, MNRAS, 310, 317

Leech, K., Kester, D., Shipman, R. et al. 2003 ESA SP–1262

Lemke, D. et al. 1996, A&A 315, L64

Li, A., Draine, B. T. 2002, ApJ 572, 232

Lonsdale-Persson C. J., Helou, G. 1987, ApJ 314, 513

Lord, S.D., Malhotra, S., Lim, T. et al. 1996, A&A, 315, L117

Lu, N., Helou, G., Werner, M. W., Dinerstein, H. L., Dale, D. A., Silbermann, N. A., et al. 2003, ApJ 588, 199

Madden, S. C., 2000, New Astr. Rev. 44, 249

Madden, S. C., Geis, N., Genzel, R., Herrmann, F., Jackson, J. et al. 1993, ApJ 407, 579

Malhotra, S., Helou, G., Hollenbach, S., Kaufman, M., Lord, S. et al. 1999, in Proceedings of the Conference "The Universe as seem by ISO", eds. Eds. P. Cox & M. F. Kessler. ESA-SP 427., p. 937

Malhotra, S., Helou, G., van Buren, D., Kong, M., Beichman, C. H., Dinerstein, H., et al. 1996, A&A 315, L161

Malhotra, S., Kaufman, M.J., Hollenbach, D., Helou, G., Rubin, R.H. et al. 2001, ApJ 561, 766

Martin, C. et al. 2005, ApJ Letters, in press

Melisse, J. P. M., Israel, F. P. 1994, A&A, 285, 51

Misiriotis A., Popescu, C.C., Tuffs, R.J., & Kylafis, N.D. 2001, A&A, 372, 775

Negishi, T., Onaka, T., Chan, K-W., & Roellig, T.L., 2001, A&A 375, 566

O'Halloran, B., Metcalfe, L., Delaney, M., McBreen, B., Laureijs, R., Leech, K., et al. 2000, A&A 360, 871

Ott, S., Siebenmorgen, R., Chartel, N., Vo, T. 2003, in Proceedings of the conference "Exploiting the ISO data archive. Infrared astronomy in the internet age", C. Gry, S. Peschke, J. Matagne, P. Garcia-Lario, R. Lorente, A. Salama (Eds.), ESA SP-511, p.159

Pagani, L., Lequeux, J., Cesarsky, D., Donas, J., Milliard, B., Loinard, L., Sauvage, M. 1999, A&A 351, 447

Pierini, D., Leech, K.J., Tuffs, R.J., Völk, H.J. 1999, MNRAS 303, L29

Pierini, D., Leech, K. J., Völk, H. J. 2003a, A&A, 397, 871

Pierini, D., Lequeux, J., Boselli, A., Leech, K. J., Völk, H. J. 2001, A&A, 373, 827

Pierini, D. & Möller, C. 2003, MNRAS 346, 818

Pierini, D., Popescu, C. C., Tuffs, R. J., Völk, H. J. 2003b, A&A 409, 907

Pfenniger, D., Combes, F. 1994, A&A 285, 94

Pfenniger, D., Combes, F., Martinet, L. 1994, A&A 285, 79

Popescu, C.C., Misiriotis A., Kylafis, N.D., Tuffs, R.J., & Fischera, J., 2000b, A&A, 362, 138

Popescu, C.C., Tuffs, R.J. 2002a, MNRAS 335, L41

Popescu, C.C., Tuffs, R.J. 2002b, Reviews in Modern Astronomy, vol 15., Edited by Reinhard E. Schielicke. Wiley, ISBN 352640404X, p.239

Popescu, C.C, Tuffs, R.J. 2003, A&A 410, L21

Popescu, C.C., Tuffs, R.J., Fischera, J., Völk, H.J. 2000a, A&A, 354, 480

Popescu, C. C., Tuffs, R. J., Kylafis, N. D. & Madore, B. F. 2004, A&A 414, 45

Popescu, C.C., Tuffs, R.J., Madore, B.F., Gil de Paz, A., Völk, H. et al. 2005, ApJ
    Letters, in press

Popescu, C.C., Tuffs, R.J., Völk, H.J., Pierini, D. & Madore, B.F., 2002, ApJ 567,
    221

Quillen, A. C., Rieke, G. H., Rieke, M. J., Caldwell, N., Engelbracht, C. 1999, ApJ
    518, 632

Reach, W. T., Boulanger, F., Contursi, A., Lequeux, J. 2000, A&A 361, 895

Rice, W., Lonsdale, C.J., & Soifer, B.T., et al. 1988, ApJS 68, 91

Roussel, H., Sauvage, M., Vigroux, L., Bosma, A. 2001a, A&A 372, 427

Roussel, H., Sauvage, M., Vigroux, L., Bosma, A., Bonoli, C., Gallais, P., et al.
    2001b, A&A 372, 406

Roussel, H., Vigroux, L., Bosma, A., Sauvage, M., Bonoli, C., Gallais, P., et al.
    2001c, A&A 369, 473

Sauvage, M., Blommaert, J., Boulanger, F., Cesarsky, C. J., Cesarsky, D. A., Desert,
    F. X., et al. 1996, A&A 315, L89

Sauvage, M., et al. 2004, in preparation.

Schmidtobreick, L., Haas, M., & Lemke, D. 2000, A&A 363, 917

Siebenmorgen, R., Krügel, E., Chini, R. 1999, A&A, 351, 495

Silva, L., Granato, G. L., Bressan, A., Danese, L. 1998, ApJ 509, 103

Smith, B. J. 1998, ApJ 500, 181

Smith, B. J. & Madden S.C. 1997, AJ 114, 138

Soifer, B.T., & Neugebauer, G. 1991, AJ, 101, 354

Stacey, G. J., Geis, N., Genzel, R., Lugten, J.B., Poglitsch, A. et al. 1991, ApJ 373,
    423

Stacey, G.J., Swain, M.R., Bradford, C.M. et al. 1999, in hte "Universe as seen by
    ISO", 1998, ESA SP-427, p. 973

Stickel, M., Bregman, J.N., Fabian, A.C., White, D.A., & Elmegreen, D.M. 2003,
    A&A 397, 503

Stickel, M., Lemke, D., Klaas, U., Beichman, C.A., Rowan-Robinson, M. et al. 2000,
    A&A 359, 865

Stickel, M., Lemke, D., Klaas, U., Krause, O., & Egner, S. 2004. A&A 422, 39

Swaters, R. A., Sancisi, R. & van der Hulst, J. M. 1997, ApJ 491, 140

Temi, P., Brighenti, F., Mathews, W..G., & Bregman, J. 2004, ApJS 151, 237

Trewhella, M., Davies, J. I., Alton, P. B., Bianchi, S., & Madore, B. F. 2000, ApJ
    543, 153

Tuffs, R.J., Lemke, D., Xu, C. et al. 1996, A&A 315, L149

Tuffs, R.J. & Gabriel, C., 2003, A&A 410, 1075

Tuffs, R.J. & Popescu, C.C. 2003, in "Exploiting the ISO Data Archive. Infrared
    Astronomy in the Internet Age", Siguenza, Spain 24-27 June, 2002. Eds. C. Gry
    et al., ESA SP-511, p. 239.

Tuffs, R.J., Popescu, C.C., Pierini, D., Völk, H. J., Hippelein, H. et al. 2002a, ApJS
    139, 37

Tuffs, R.J., Popescu, C.C., Pierini, D., Völk, H. J., Hippelein, H. et al. 2002b, ApJS
    140, 609

Tuffs, R.J., Popescu, C. C., Völk, H.J., Kylafis, N.D., & Dopita, M.A. 2004, A&A
    419, 821

Uchida, K. I., Sellgren, K., Werner, M. W., Houdashelt, M. L. 2000, ApJ 530, 817

Valentijn, E. A., van der Werf, P. P. 1999a, in Proceedings of the Conference "The
    Universe as seem by ISO", Eds. P. Cox & M. F. Kessler. ESA-SP 427., p.821

Valentijn, E. A. & van der Werf, P. P. 1999b, ApJ 522, L29

Valentijn, E. A., van der Werf, P. P., de Graauw, Th., de Jong, T. 1996, A&A 315, L145

van Dishoeck, E. F., 2004 ARA&A, in press

Völk, H.J., & Xu, C. 1994, Infrared Physics and Technology, 35, 527

Vogler, A., Madden, S. C., Beck, R., Sauvage, M., Vigroux, L., Ehle, M., 2004, *in preparation*

Walsh, W., Beck, R., Thuma, G., et al. 2002, A&A 388, 7

Wilke, K., Klaas, U., Lemke, D., Mattila, K., Stickel, M., et al. 2004, A&A 414, 69

Wilke, K., Stickel, M., Haas, M., Herbstmeier, U., Klaas, U., et al. 2003, A&A 401, 873

Wunderlich, E., Klein, U. 1988, A&A 206, 47

Wunderlich, E., Wielebinski, R. & Klein, U. 1987, A&AS 69, 487

Xilouris, E. M., Madden, S. C., Galliano, F., Vigroux, L., Sauvage, M. 2004, A&A 416, 41

Xu, C. & Buat, V. 1995, A&A 293, L65

Young, L.M. & Lo, K.Y. 1997, ApJ 476, 131